catalysts

MDPI

Review

Switchable Intrinsic Defect Chemistry of Titania for Catalytic Applications

Swaminathan Jayashree [1,2] and Meiyazhagan Ashokkumar [1,*]

[1] Department of Materials Science & NanoEngineering, Rice University, Houston, TX 77005, USA; jayashreesavithiri@gmail.com

[2] CSIR-Central Electrochemical Research Institute, Karaikudi 630003, India

* Correspondence: ma37@rice.edu; Tel.: +1-713-348-5456

Received: 23 October 2018; Accepted: 18 November 2018; Published: 2 December 2018

Abstract: The energy crisis is one of the most serious issue that we confront today. Among different strategies to gain access to reliable fuel, the production of hydrogen fuel through the water-splitting reaction has emerged as the most viable alternative. Specifically, the studies on defect-rich TiO_2 materials have been proved that it can perform as an efficient catalyst for electrocatalytic and photocatalytic water-splitting reactions. In this invited review, we have included a general and critical discussion on the background of titanium sub-oxides structure, defect chemistries and the consequent disorder arising in defect-rich Titania and their applications towards water-splitting reactions. We have particularly emphasized the origin of the catalytic activity in Titania-based material and its effects on the structural, optical and electronic behavior. This review article also summarizes studies on challenging issues on defect-rich Titania and new possible directions for the development of an efficient catalyst with improved catalytic performance.

Keywords: Titania defect; defect classifications; Titania; catalysis; electron-hole; vacancy; defect chemistry; water-splitting

1. Introduction

Some of the world's technologies are currently due to the manipulation of defects. For example, defects can transform a hard white solid α-Al_2O_3 (corundum) to colored gems like ruby and sapphire [1]. Thus, the intentional creation of defects in materials with control over their concentration, type, spatial distribution, and location can drastically modify their functionalities. In particular, defect engineering serves as a platform to tailor the intrinsic electrons of materials and, hence, to tune their properties, reactivity, and catalytic activity [2–13]. The past centuries have witnessed significant progress towards commercialization of water-splitting technologies predominantly due to the intentional creation of defects in various catalytically in-active materials [14–22], but still, we are distant from the basic understanding of structural defects and the critical parameters which play an essential role in water-splitting applications. The grand challenge lies in the development of an improved catalyst for water-splitting applications. A stream of research focuses only on the effect of intrinsic defects on the solid-state properties of the material [23–35]. Few other groups concentrate on improving the electronic, optical properties of materials and discussing issues related to water-splitting reaction [36,37]. However, the progress of water electrolyzer technology requires combining these two research areas in order to address the challenges in developing an enhanced catalyst for water-splitting. Hence, it is a desperate need to fully understand the role of defect disorder on water-splitting in order to enhance the performance of electro/photocatalyst for water-splitting reaction.

To understand the scientific origin of catalytic activity on the disordered structures herein, we focus our interest on: (i) defects and defect chemistry; (ii) standard experimental approaches to

generate point defects; (iii) the effect of having defects on their structural, electrical, optical behavior and, hence, catalytic activity; (iv) role of defects associated with the electrocatalytic production of hydrogen and photo-oxidation of water; and (v) challenges and applications of defect-rich Titania. Along with this, we have included perspectives and outlook on the future of the defect engineering. Several reports and reviews exist summarizing various statements on defect-engineered catalyst for water-splitting reaction [38–42]. Hence, in this review, we attempted to articulate the impact of defects on the structural, optical and electronic properties, which are critical factors for defining the catalytic activity of a material. We believe that a fundamental understanding of the defect engineering and combination of optimization strategies would be the bottleneck for finding the appropriate candidates for water-splitting reaction. Notably, we collectively discussed intrinsic defect engineering (self-doping) of futuristic catalyst 'Titania' for water-splitting reaction. The striking characteristics of Titania such as strong oxidizing power, earth abundance, non-toxic, chemical, physical and thermal stability, easy availability and excellent photoactivity supports this material as the best option for water-splitting reaction. It is also a ninth earth abundant material, obtained from the mineral ilmenite [43,44], and its phase diagram (Figure 1) shows various stable phases at different Ti/O stoichiometry.

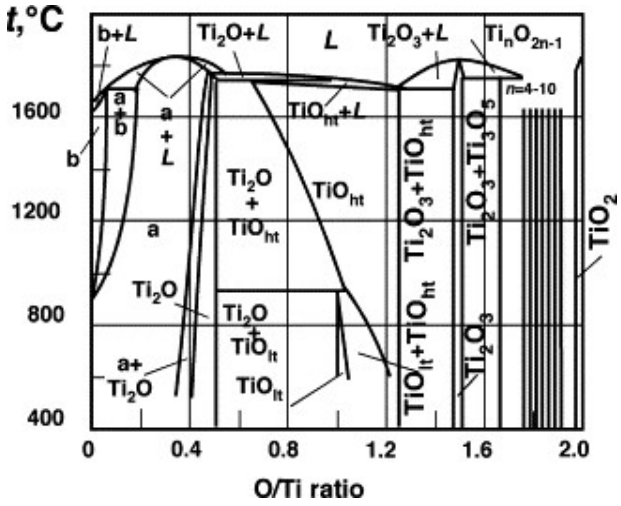

Figure 1. Phase diagram of the Ti-O system. The region Ti_2O_3-TiO_2 contains Ti_3O_5, Ti_2O_3 and seven discrete phases of the homologous series Ti_nO_{2n-1} (Magneli phase) and TiO_2. Reproduced from [35]; Copyright 2003, Elsevier.

2. Defects in Titania

In general, four common native-point defects (Figure 2) exist in Titania: (i) Oxygen vacancies (V_o)—Missing of oxygen ion from the lattice site; (ii) Titanium vacancies (V_{Ti})—Ti ion is missing from its lattice site; (iii) Titanium interstitials (Ti_i)—Ti ion is located in an interstitial site; and (iv) Oxygen interstitials (O_i)—Oxygen ion is located in an interstitial site.

General characteristics of point defects in Titania/Defect chemistry of Titania:

(i) Point defects preferably gather as clusters rather than distributed randomly on the crystal structure and, hence, lead to line defects, planar and volume defects [45].

(ii) Depending on the location of defects in the crystal structure, the activity varies as tabulated in Table 1.

(iii) Point defects are generally represented using Kroger-Vink notation (Table 2).

(iv) As charge-neutrality demands, point defects usually form as a charge-neutral complexes [Schottky defects (e.g., $V_{Ti}^{\bullet\bullet\bullet\bullet} + 2V_O^{\bullet\bullet}$, $2Ti_{Ti}^{\bullet} + V_O^{\bullet\bullet}$) and Frenkel defects (e.g., $O_{Ti}'' + V_O^{\bullet\bullet}$, $V_{Ti}'''' + Ti_i^{\bullet\bullet\bullet\bullet}$)]. Their formation defect equilibria are given below [48,49]:

(1) Defect equilibria of oxygen vacancy (V_O) formation: $O_o \Longleftrightarrow V_o^{\bullet\bullet} + 2e' + \frac{1}{2} O_2$

(2) Defect equilibria of Titanium vacancies (V_{Ti}): $O_2 \Longleftrightarrow 2O_o + V_{Ti}^{\bullet\bullet\bullet\bullet} + 4h^{\bullet}$

(3) Defect equilibria of Titanium interstitials (Ti_i): $2O_o + Ti_{Ti} \Longleftrightarrow Ti_i^{\bullet\bullet\bullet} + 3e' + O_2$

(4) Defect equilibria of oxygen interstitials (O_i): $V_i^x + \frac{1}{2} O_2 \Longleftrightarrow O_i'' + 2h^{\bullet}$

(V) Intuitively, ionization of these ionic defects leads to the formation of electronic defects in the crystal system, which are called color centers [50,51]. There are two types of color center-based on their charge (i) electron center (F) and (ii) electron-hole center (V) and classified further as F, F^+, F^{++} and V, V^+, V^{++}, respectively.

Table 1. Behavioral difference of defects in the bulk and the surface [46].

Bulk	Surface
Interstitial atom	Adatom
Vacancy	Vacancy
Interstitial Cluster	Adatom island
Vacancy Cluster	Vacancy island
Kick-in/Kick-out	Exhange diffusion
Vacancy-interstitial formation	Vacancy-adatom formation

Table 2. Kroger-Vink notation and their meaning [47].

Kroger-Vink Notation	Meaning
$Ti_i^{\bullet\bullet\bullet}$	Ti^{3+} ion in the interstitial site
$Ti_i^{\bullet\bullet\bullet\bullet}$	Ti^{4+} ion in the interstitial site
$V_o^{\bullet\bullet}$	Oxygen vacancy
O_i''	O^{2-} ion in the interstitial site
V_{Ti}''''	Titanium vacancy

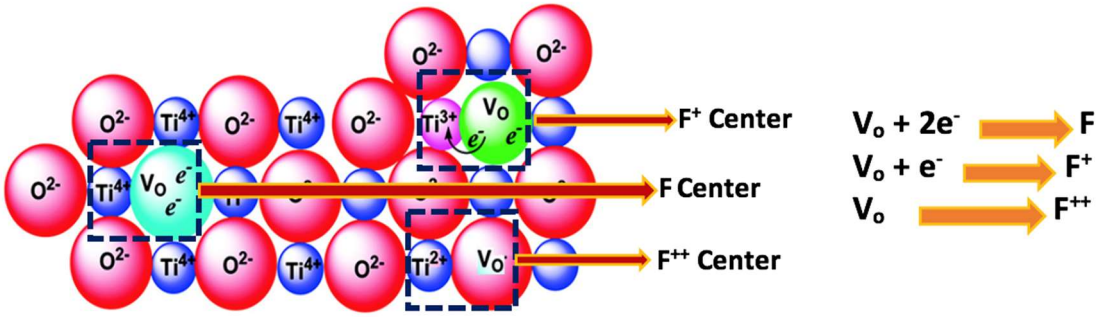

Figure 2. Schematic illustration and description of F center formation in Titania. Reproduced from [52], Copyright 2009, American Chemical Society.

2.1. Electron (F, F^+, F^{++}) Center

This center occurs due to the absence of a negatively charged ions (i.e., oxygen vacancy) in Titania. As a result of charge imbalance, it possess positive charge and, hence, attracts, traps electron and comprises F centers [52,53].

2.1.1. F Center

The vacancy of oxygen (V_o) is compensated by a pair of unpaired electrons from Ti 3d orbitals, resulting in a (double) positive charged vacancy (F center). It has four Ti^{4+} ions in the neighborhood with no unpaired electrons.

2.1.2. F^{+} Center

One of the electrons from F center tends to occupy the neighborhood Ti^{4+} ion, so it is positively charged with respect to the lattice, yields $Ti^{3+}_{lattice}$ center (F^{+} center). It possesses one unpaired electron.

2.1.3. F^{++} Center

Both electrons from F center tend to occupy the neighboring Ti^{4+} ion, so it is positively charged with respect to the lattice and yield $Ti^{2+}_{lattice}$ center (F^{++} center).

The formation mechanism and defect equilibria are shown below (Figure 2):

2.2. Electron Holes

It is an antimorph of F center [54], consisting of Titanium vacancy and holes, which gives p-type conductivity to Titania as shown in Figure 3.

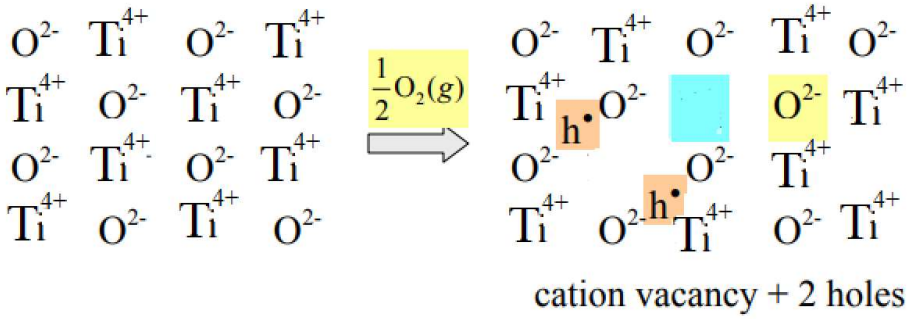

Figure 3. Electron-hole formation mechanism.

These point defects possess distinct energy and, therefore, have different formation energies [55]. Recently, formation energy of various defects in Titania has been calculated as a function of fermi energy since fermi level of a material is based on their charged defects, electron and hole carriers (Figure 4a,b) [56]. According to them, the formation of the surpassing defect type in Titania depends upon their non-stoichiometry level. At Ti-rich conditions, titanium interstitials and oxygen vacancies are formed, and they behave as weak donors. While the formation of titanium vacancy is favored at O-rich growth conditions, they act as deep acceptors. M. K. Nowotny et al. attempted methods to derive the defect disorder diagram of Titania as a function of oxygen partial pressure (Figure 4c) including illustrating the concentration of specific defects at different oxygen partial pressure [57]. Under low oxygen pressure/activity, a considerable reduction of Titania leads to the formation of titanium interstitials (Ti excess: Ti_{1+x} O_2) and electrons. While at prolonged oxidizing conditions, titanium vacancies with electron holes (acceptors) may become as most dominant defects. Hence, the predominant defect in Titania over a wide range of stoichiometry (under strongly reduced, reduced and oxidized conditions) is oxygen vacancies (donors) and it is compensated by ionic charge (electrons). It is also supported by Kofstad, 1972 (Figure 5d). Thus, oxygen vacancies and titanium interstitials mostly dominate the defect chemistry of Titania due to their lower formation enthalpies and it leads to n-type conductivity in Titania. Formally, titanium vacancies are thermodynamically reversible defects (theoretically); hence, they are usually obtained by quenching to make it as an irreversible defect [58–63].

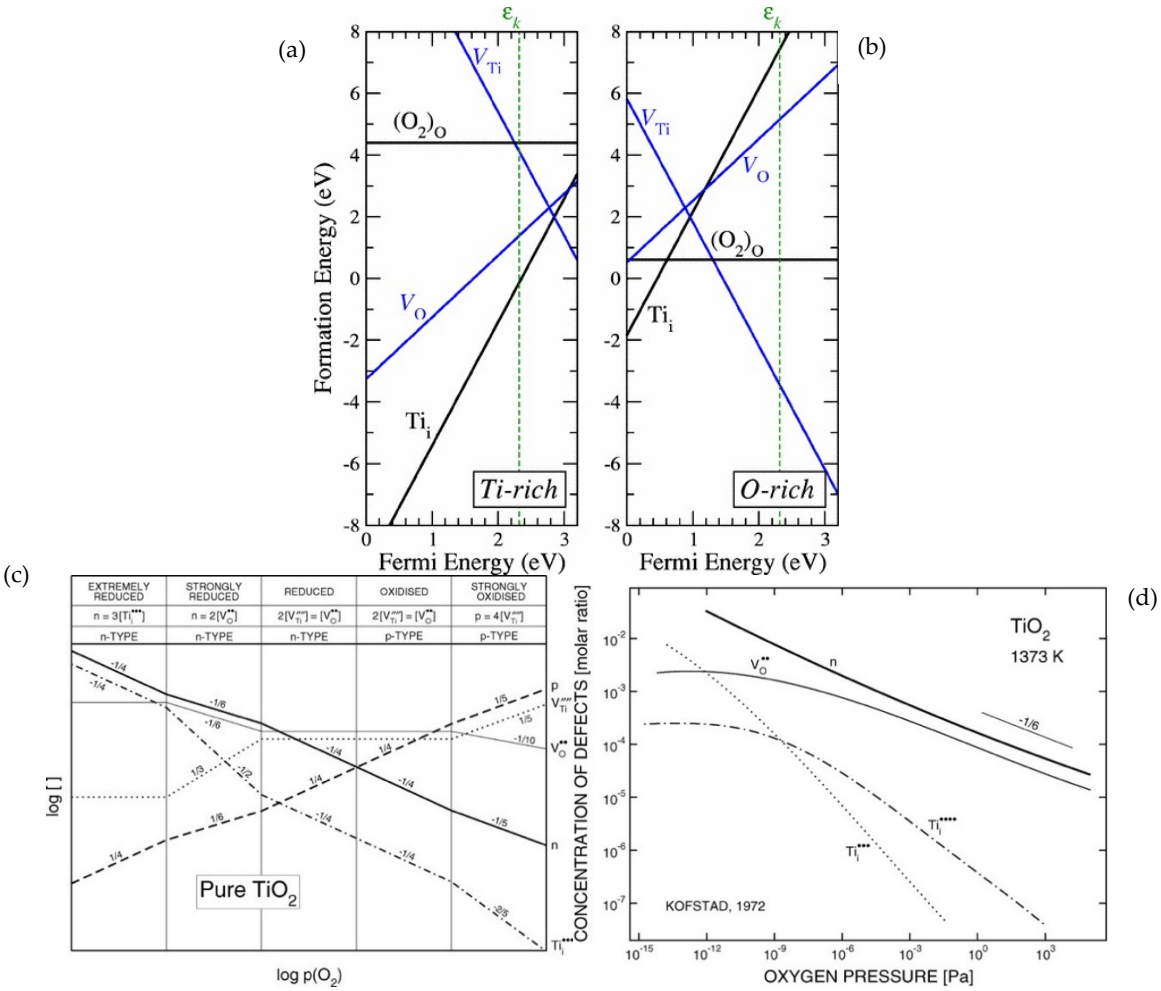

Figure 4. (**a**) DFT—calculated defect formation energies in Titania as a function of fermi energy (E_F) under Ti-rich and (**b**) O-rich growth conditions. Reproduced from [56], Copyright 2006, The American Physical Society. (**c**,**d**) Variation in defect concentration under different oxygen pressure conditions [57,58]. Reproduced from [57], Copyright 2008, American Chemical Society.

Based on the above discussion, it is understood that an appropriate growth condition is required to incorporate the required defects in Titania. It is also a challenge to integrate particular defects, since various complexities involve in the formation of defects.

3. Experimental Approaches to Generate Defects in Titania

The defects in Titania are induced either by an in-situ control (defects creation during synthesis or ex-situ controlled (the incorporation of defects after preparation) mechanism. The reported methods to produce Ti interstitial in Titania are prolonged oxidation (1000 °C for 24 h) [60,64–67]. The state-of-the-art method to prepare reduce Titania (oxygen deficient) include energetic ion or electron beam implantation, UV irradiation, heating TiO_2 under vacuum, thermal annealing to high temperatures (above 500 K), reducing conditions (C, H_2), plasma-treating, laser, and high-energy particle (neutron, Ar^+, electron, or γ-ray) bombardment, chemical vapor deposition, vacuum activation, metal reduction, electrochemical reduction, partial oxidation starting from Ti, Ti(II) and Ti(III) precursors, etc. [68–83].

In general, the sequence of reduction of TiO_2 is:

$$TiO_2 \rightarrow Ti_nO_{2n-1}\ (n > 10) \rightarrow Ti_nO_{2n-1} (4 < n < 10) \rightarrow Ti_3O_5 \rightarrow Ti_2O_3 \rightarrow TiO \rightarrow Ti_2O$$

Hence, defect formations and their concentration, as well as the properties depend on the preparative conditions. The design of synthesis with defects also has a significant effect on the intrinsic properties such as structural, electrical, optical behavior and, in turn, their catalytic activity.

3.1. Effect of Defects on Crystal Structure of Titania

Point defects in Titania will induce lattice relaxation and ionic polarization effect, and, hence, affect the surface geometries (i.e., atomic arrangement and coordination) [84–86]. Upon removal of the O atom, the nearest Ti–Ti bonds tend to relax away from the vacancy in order to reinforce their bonding with rest of the lattice. Simultaneously, the neighboring Ti–O bonds displace slightly inwards due to the electrostatic attraction induced by oxygen vacancies. This internal modulation induced by oxygen vacancy defects result in the rearrangement of atomic positions and decreases the overlap between Ti dangling bonds closer to the vacancy, and consequently leads to a reduction in Ti–O bond length [87–89]. This defect creates uneven internal stress/strain and leads to distortion in TiO_6 octahedra, which diverges with the concentration of defects and constitutes the material with different octahedral packing and crystal symmetry [90] as depicted by E. Stoyanov et al. (Figure 5).

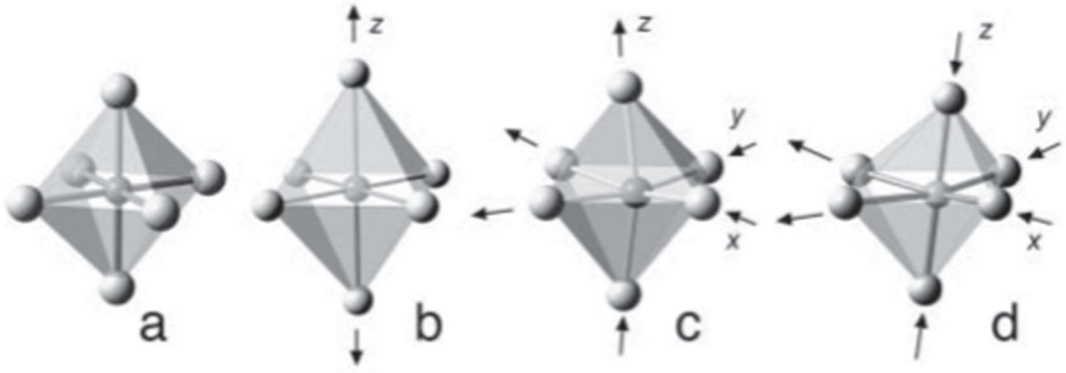

Figure 5. Different types of octahedral packing (**a**) no distortion (cubic TiO), (**b**) tetragonal distortion(rutile) (**c**) trigonal distortion (Ti_2O_3) (**d**) orthorhombic- like distortion (Ti_4O_7 and Ti_5O) Reproduced from [90], Copyright 2007, American Mineralogist.

As the concentration of oxygen vacancy defects increases, ordering of vacancy occurs, and it leads to the formation of new phases of titanium oxide, (i.e., Structural condensation happens to avoid having entire layers of vacant sites and form extended planar defects [crystallographic shear (CS) planes] with random or regular spacing) [91,92]. The number of CS planes increases thickness of the blocks as well between adjacent CS planes decreases with an increase in vacancy [90].

3.2. Crystal Structures of Various Titanium Oxides

Stoichiometric Titania (TiO_2) exists as a well-known phase such as rutile (tetragonal-$P4_2/mnm$), anatase (tetragonal-$I4_1/amd$) and brookite (orthorhombic-Pbca). Whereas the structure of non-stoichiometric Titanium oxide varies with O/Ti stoichiometry as summarized in Figure 6 and Table 3.

Crystal structures of some well-known Ti oxides are discussed below:

Titanium dioxide (TiO_2): The crystal structure of TiO_2 is considered as a two-dimensional chain of edge-sharing TiO_6 octahedra with individual chains linked at a corner oxygen atom to form the 3D lattice. Each octahedron is made up of titanium atom at the center and oxygen at each corner.

$$\text{Magneli phase} - Ti_nO_{2n-1}\ (n = 4\text{–}10)\ (\text{e.g., } Ti_4O_7,\ Ti_5O_9,\ Ti_6O_{11}\ \ldots\ )$$

The crystal structure of Magneli phases is made of TiO_2 octahedra blocks with an oxygen vacancy at every n^{th} layer, which leads to shear planes in the structure as illustrated in Figure 7. The TiO_2

octahedra blocks are coupled via edges and corners while shear planes have face-sharing octahedral. This atomic arrangement leads to titanium-atom positions in one block which matches with the interstitial or unoccupied positions in the next block. This organization ultimately decreases the symmetry of the crystal system from tetragonal to triclinic as the size of the unit cell increases.

Table 3. Variation of the crystal structure with O/Ti stoichiometry.

Compound	X in TiO_x	Structure
TiO_2	2	Rutile
$Ti_{10}O_{19}$	1.9	Anatase
Ti_9O_{17}	1.89	Triclinic
Ti_8O_{15}	1.875	Triclinic
Ti_7O_{13}	1.857	Triclinic
Ti_6O_{11}	1.833	Triclinic
Ti_5O_9	1.8	Triclinic
Ti_4O_7	1.75	Triclinic
γTi_3O_5	1.67	Monoclinic
Ti_2O_3	1.5	Tetragonal
TiO	1.0	Hexagonal Cubic Monoclinic
Ti_2O	0.5	Hexagonal
Ti	0	Hexagonal

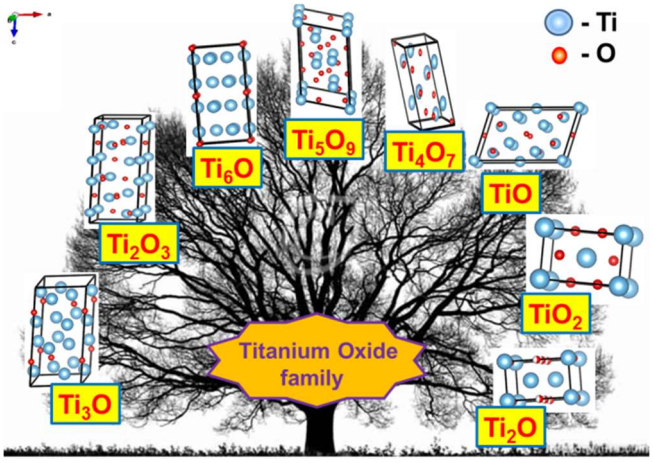

Figure 6. Crystal structures of various titanium oxides.

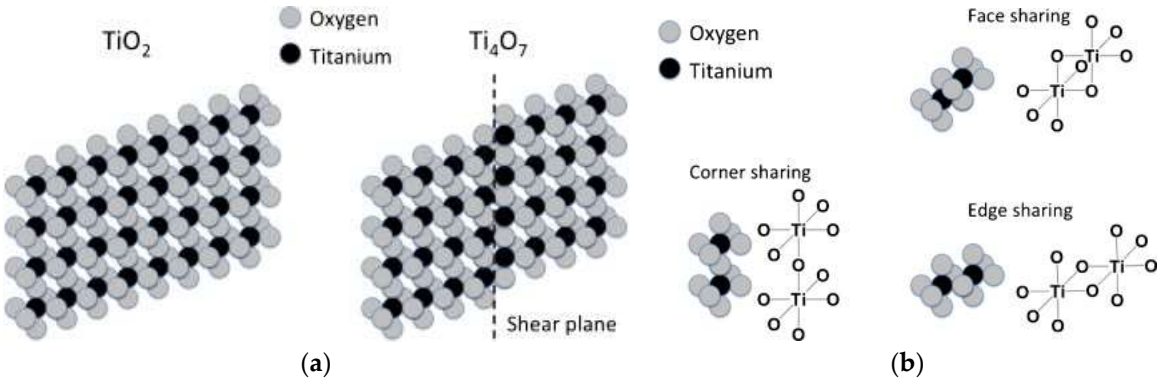

Figure 7. (**a**) Difference between TiO_2 and Ti_4O_7 (Magneli phase) structure (**b**) Different orientations of TiO_2 octahedra in Magneli phase materials. Reproduced from [92], Copyright 2010, Elsevier.

◊ The structure of magneli phase can be regarded as made of stacked alternating shear slabs and the family members of magneli phase differ in many shear planes. Thus, they also diverge in length of the pseudo-rutile chain segments.

◊ Magneli phases with higher n value possess greater shear plane interval. The shear planes provides a pathway for electrons transport, and hence, magneli oxides are an excellent electrical conductor [93].

◊ Magneli phase is a mixed valence compound of (n−2) Ti^{4+} ($3d^0$) and two Ti^{3+} ($3d^1$) configurations. The presence of both Ti^{3+} and Ti^{4+} ions offer several possible configurations of Ti in the crystal, leading to various charge-ordered states and viewed as electron-doped (oxygen deficient) TiO_2 [94].

◊ The value of n assures the crystal structure as well the electronic structure of the Magneli phase.

Ti_3O_5: The unit cell includes two Ti^{3+} ions and one Ti^{4+} ion with a different significant Ti–O distance leading to a distorted octahedron [95,96].

Ti_2O_3: The stoichiometry of Ti_2O_3 extends from $TiO_{1.49}$ to $TiO_{1.51}$ and comprises pairs of Ti^{3+} ions in octahedral sites as a fundamental component in the unit cell [97,98].

TiO:

Δ TiO has a defective NaCl structure (space group $Fm\bar{3}m$) and possesses 10–15 at % vacancies at both Ti and O sites [99]. Owing to higher structural vacancies in titanium monoxide, they are considered as strongly non-stoichiometric and has a broader homogeneity region from $TiO_{0.70}$ to $TiO_{1.25}$ [100,101].

Δ TiO has two polymorphs based on the vacancy distribution. If the vacancies are randomly distributed it leads to disordered cubic phase, and the other polymorph has ordered vacancies with monoclinic symmetry [83,102–106].

Δ It is metallic in nature due to the high content of vacancy channels [107].

Ti_2O:

Δ Ti_2O has anti-CdI_2 structure and consists of zigzag oxygen rows with alternate O layers vacant. It possesses more antiphase boundaries and stacking faults [108–111].

Based on the above discussion, it infers that striking changes in the crystal structure of titanium oxides have occurred due to the relatively small structural alterations through defects.

4. Effect of Defects on Optical Behavior of Titania

Stoichiometric TiO_2 is a wide bandgap semiconductor (3.3 eV), and, hence, it absorbs UV light, while reduced Titania absorbs visible light and behaves as a semiconductor or metal depending on their oxygen vacancy (Figure 8) [74,112–119].

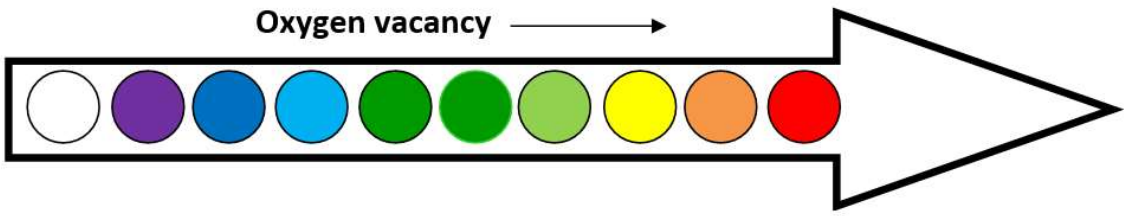

Figure 8. Enhancement of visible absorption with increasing oxygen vacancy.

According to crystal field splitting (Figure 9), Ti (3d, 4s, 4p) orbitals are linearly coalesced with O (2s, 2p) orbitals to form molecular orbitals as depicted in Figure 9 [90]. The upper t_{2g}* and, eg* are primarily of Ti 3d character and configure conduction band, while the lower t_{2g} and, e_g are mainly of O 2p character and form valence band, respectively [90].

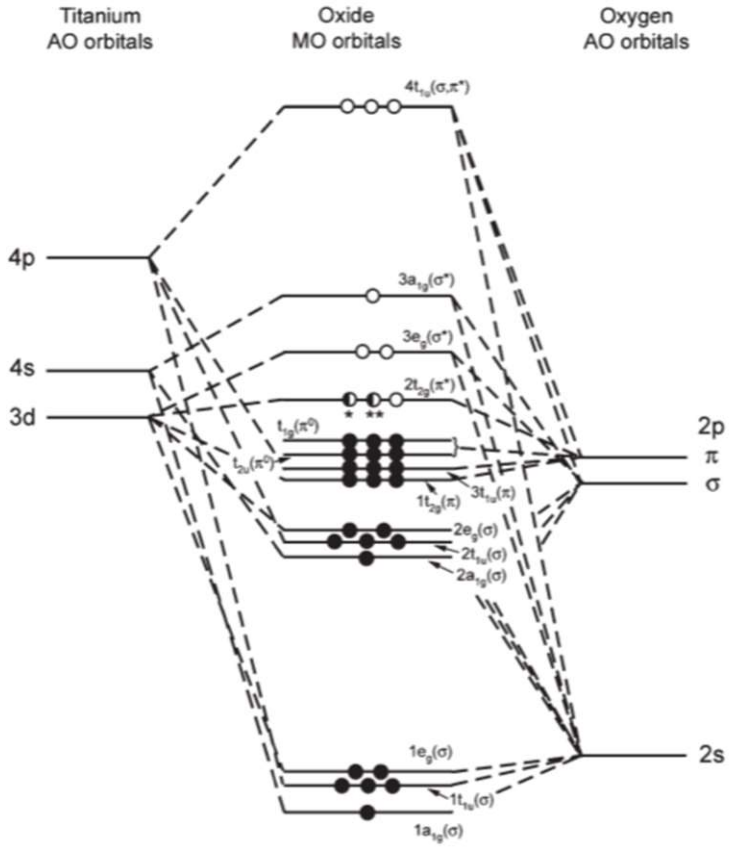

Figure 9. Molecular orbital diagram of TiO_2, Ti_2O_3, TiO. Reproduced from [90], Copyright 2007, American Mineralogist.

The defects and non-stoichiometry in reduced Titania will induce alterations in Ti 3d occupancies and directly control the local structure of t_{2g} and, e_g orbitals due to Jahn-Teller effect. The following difference in the splitting of t_{2g} and e_g levels in different distorted environments of Titania are illustrated in Figure 10 [90].

As an outcome, the incorporated modifications in the crystal field as a function of increasing oxygen vacancy content are:

- the systematic decrease in crystal field splitting between t_{2g} and, e_g levels.
- the covalent bonding between Ti and O becomes ionic.
- The degree of electron occupancy in the t_{2g} level increases. TiO_2 has none, Ti_2O_3 has one and TiO has two t_{2g} electrons.

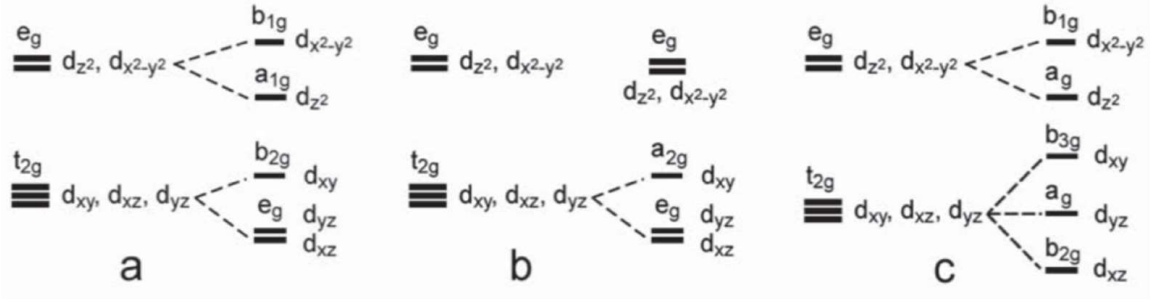

Figure 10. Splitting of t_{2g} and, e_g levels in tetragonal (**a**), trigonal (**b**), and orthorhombic (**c**) distorted environments. Reproduced from [90], Copyright 2007, American Mineralogist.

Besides the above-described changes in crystal symmetry and coordination number, the extent of mixing of Ti 3d and O 2p orbitals is also affected, and, hence, their electronic band structure and band gap vary on titanium oxide polymorphs. It is also known that the oxygen vacancy and titanium interstitial behave as donor states since their energy level is closer to the conduction band; while titanium vacancy forces the Fermi level towards the valence band, to accept electrons from their surrounding O atoms and act as an acceptor state [49,120–125]. The distinct energy levels of various defect states in titanium oxide are shown in Figure 11 [86].

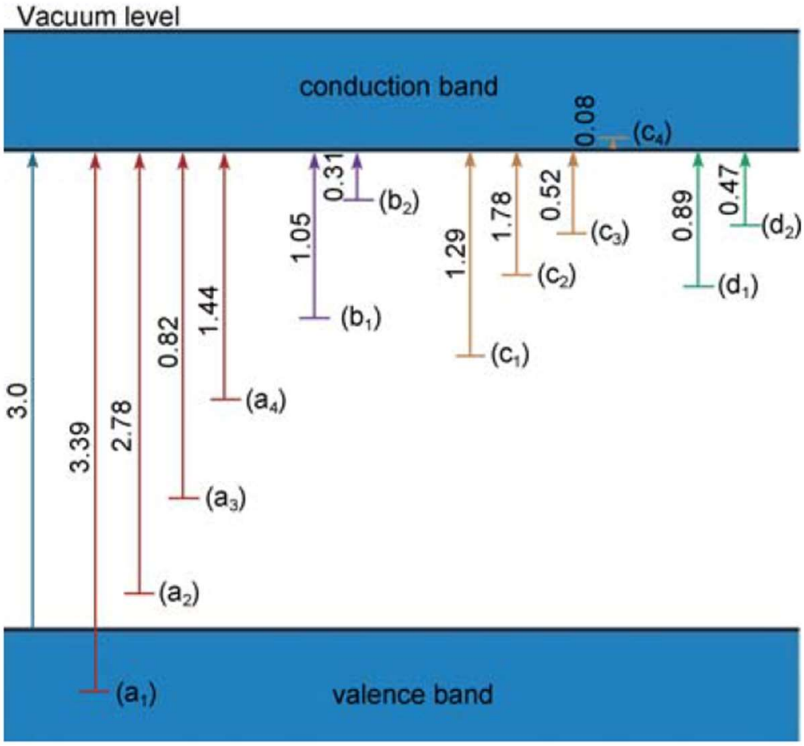

Figure 11. Various defect levels of Titania. The numbered letters a_1, a_2, a_3, a_4, b_1, b_2, c_1, c_2, c_3, c_4, d_1 and d_2 represent the defect levels $V_{Ti}^{x}/V_{Ti}^{\bullet}$, $V_{Ti}^{\bullet}/V_{Ti}^{\bullet\bullet}$, $V_{Ti}^{\bullet\bullet}/V_{Ti}^{\bullet\bullet\bullet}$, $V_{Ti}^{\bullet\bullet\bullet}/V_{Ti}^{\bullet\bullet\bullet\bullet}$, O_o'/O_i'', O_o^{x}/O_i', $Ti_i^{\bullet\bullet\bullet}/Ti_i^{\bullet\bullet\bullet\bullet}$, $Ti_i^{\bullet\bullet}/Ti_i^{\bullet\bullet\bullet}$, $Ti_i^{\bullet}/Ti_i^{\bullet\bullet}$, $Ti_i^{x}/Ti_i^{\bullet}$, $V_o^{\bullet}/V_0^{\bullet\bullet}$ and $V^{x}/V^{\bullet}$, respectively [86]. Reproduced from [86], Copyright 2011, Science China Press and Springer-Verlag Berlin.

With these continuous formations of defect states, localized midgap states in between the bandgap will enrich and ultimately narrow the band gap of TiO_2. Thus, the formation of vacancies results in shifts of average band energies, change of band widths and position of the Fermi level with the creation of new "vacancy states" in the bandgap. It also formulates an accumulation layer in the near-surface region that leads to a downward band bending [126].

The structural model of certain reduced Titania with their characteristic optical behavior and preparation methods are illustrated in Figure 12 [127]. As seen in Figure 12, Ti and O reside in their lattice and give rise to a colorless compound in case of stoichiometric Titania (TiO_2). While on heat treatments under the H_2 atmosphere, the surface oxygen vacancies are created and spread into bulk, which resulted in a pale blue color of a crystal. On continuing the heat treatment further, some oxygen vacancies co-exist with the conduction electrons in dark blue and dark green crystals, whereas, the conduction electrons completely migrate to the oxygen vacancy site on extensive heat treatment under the N_2 atmosphere, so that the crystal appears yellow in color. Thus, different defect concentration in reduced titanium oxide forms colorful titanium oxide.

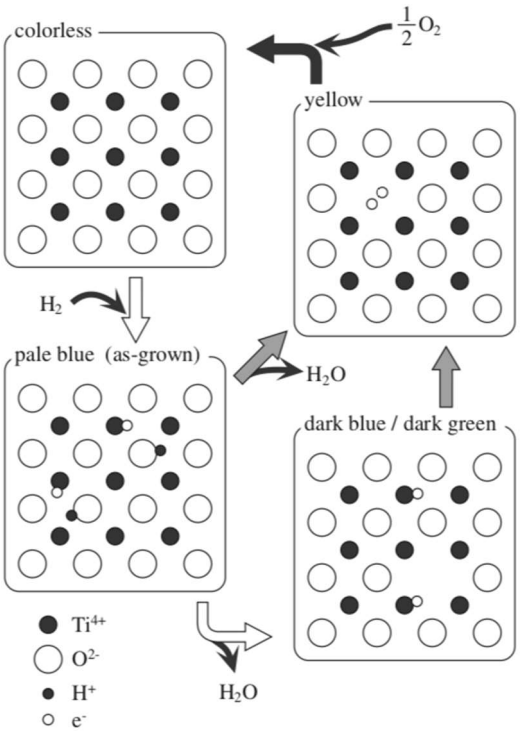

Figure 12. Schematic representation of the structural model for defect states in reduced Titania with their characteristic optical behavior and preparation methods. White, grayish and black arrows represent heat-treatments under hydrogen, inert and oxygen atmosphere, respectively. Reproduced from [127], Copyright 2004, The Physical Society of Japan.

5. Effect of Defects on Electrical Behavior of Titania

Defects turn Titania from semiconductor to metallic depending on the intensity or level of structural deformation. Usually, lower oxides of titanium are metallic conductors while higher oxide content is semiconductor or insulator. This transition of conductivity from electronic conduction in titanium to a hopping mechanism in Titania is due to the presence of oxygen. At lower oxygen content, the corresponding Ti atoms are under great proximity and interact electronically, which leads to good conductivity [128,129]. Besides, the shear planes in magneli's phase offer easy access for the charge transport and hence improvement in the conductivity as shown in Figure 13a [130]. The relative variation in conductivity of magneli's phases due to the variation in oxygen vacancy content (shear planes) is shown in Figure 13b [92].

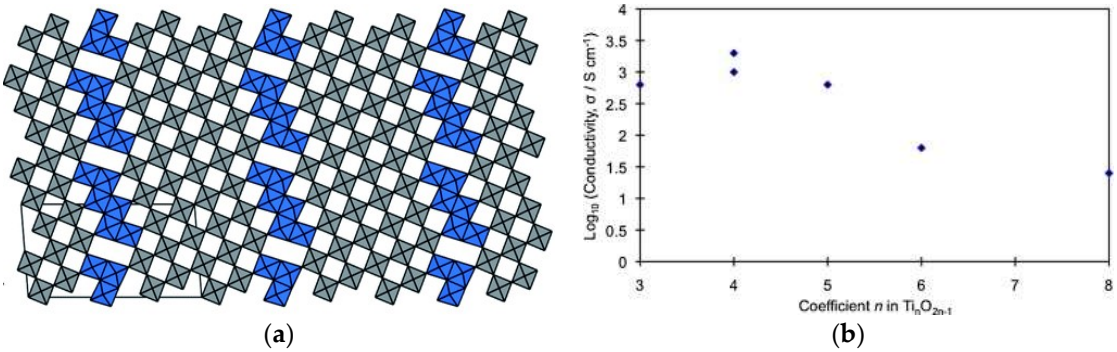

(**a**) (**b**)

Figure 13. (**a**) Magneli shear planes providing access for electrons transport. Reproduced from [130], Copyright 2014, Royal Society of Chemistry. (**b**) Relative electrical conductivities of Magneli phase titanium sub-oxides. Reproduced from [92], Copyright 2010, Elsevier.

J. Nowotny et al. described a transition from n-type to p-type conductivity in Titania under different oxygen activity conditions (Figure 14) [49]. These distinctly different electronic behaviors of reduced Titania under different oxygen activity conditions are due to the prevalence of predominant defects and due to self-structural modification.

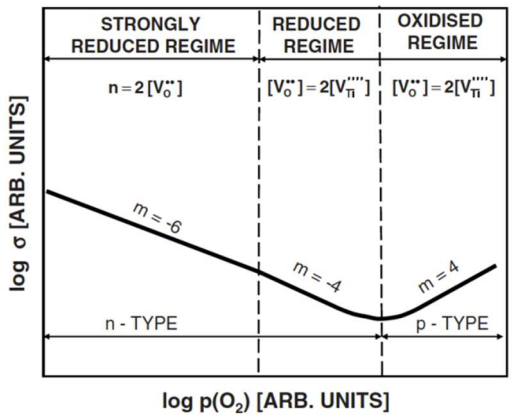

Figure 14. Effect of oxygen activity on the electrical conductivity of Titania. Reproduced from [49], Copyright 2007, John Wiley and Sons.

J. Nostalt et al. reported predominant defects and their corresponding conductivity at different oxygen abundance by the slope (m) (Table 4) [131]. The change in electrical properties at different oxygen proportions is due to the dissimilarity in electron occupancy, bond type, strength of interplay between Ti 3d orbitals and interaction between Ti 3d and O 2p orbitals (i.e., the complex interaction of charge order, orbital order). Subsequently, the electrons delocalization on different Ti ions or localized onsimilar Ti ions, which eventually leads to enhanced conductivity.

Table 4. Predominant defects and conductivity of Titania depending on the oxygen activity. Reproduced from [131], Copyright 1996, Elsevier.

m	Predominant Defects	Conductivity Type
6	$V_0^{\bullet\bullet}$, e	n
4	$V_0^{\bullet}$, e′	n
5	Ti_i^{4+}, Ti_i^{3+}, e′	n
∞	$h^{\bullet}$	p
5	V_{Ti}^{4-}, $h^{\bullet}$	p

6. Effect of Defects on the Catalytic Activity of Titania

Point defects in Titania act as catalytically active sites due to the vacancy-electron, vacancy-vacancy interactions, and vacancy-strain coupling. Furthermore, clusters of vacancy and associative vacancy voids behave as a transfer station for atom exchange or migration because of their associated 'conducting vacancy channels' and plays a governing role in the catalytic activity. Also, the vacancy-induced electrons on defective Titania are localized on the Ti atom and accelerate local lattice distortion, constituting a polaron [132]. These mobile polarons form movement with low activation energy and favor conductivity and catalytic activity [133]. Besides, a large number of donor/acceptor defect states and a large density of dangling bonds in reduced Titania cause high surface activities and provide cooperative electrical effects (e.g., improved electron transfer and transport) for catalytic activity [134]. Further, defects induce an internal stress/strain, which is crucial for faster kinetics and favorable reactivity [135,136]. Plus, point defects have a potential to stabilize the binding of surface adsorbed species and escort to stiffer molecule-surface interactions which enhance the activity. Thus, these defect-related interface effects and defect-mediated charge migration effects augment the catalytic activity towards water-splitting [70,137–143].

7. Role of Defects towards Electro-Catalytic Water Splitting

Point defects in reduced Titania build a lattice strain in the material, which induces hydrophilicity on their surface than that of (defect-free) Titania without strain [140]. Hence, water molecules are dissociatively adsorbed on the defect sites, and consequently, the number of bridging/terminal hydroxyl groups increases with increasing concentration of structural defects in reduced Titania. This hydroxyl group depresses the O^+ yield (Knotek−Feibelman mechanism) and favors lateral long-range redistribution of defect-electrons on the surface [144]. Thus, surface chemistry and electrical behavior of Titania are modified by electrons associated with oxygen vacancy defect sites and hence catalytic activity. The mentioned K-F process inversely decays with the oxygen vacancy content (Figure 15).

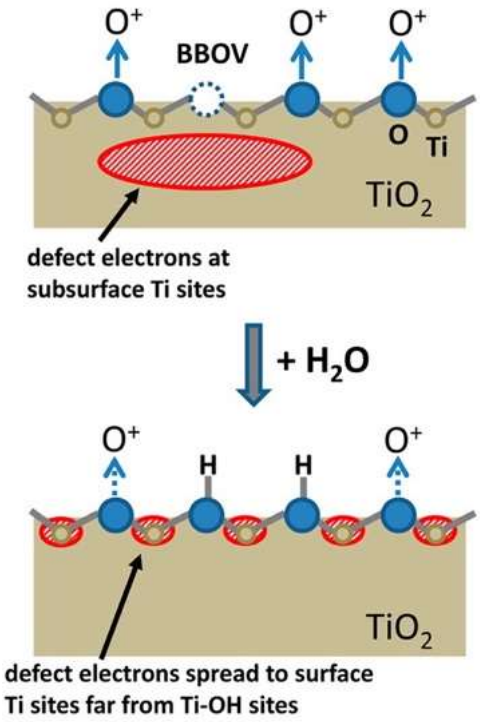

Figure 15. Influence of point defects in reduced Titania on their electronic structure. Reproduced from [144], Copyright 2013, American Chemical Society.

Similarly, titanium vacancy offers favorable active sites for water-splitting as it possesses strong electron affinity, which allows effective charge transfer for oxygen evolution reaction [57]. Hence, overall water-splitting is possible with n- and p-type defective Titania.

8. Role of Defects towards Photoelectrochemical Water Splitting

In principle, efficient photoelectrochemical watersplitting requires proficient separation of photo-generated charge carriers (photon activation) and subsequent faster transportation to the semiconductor interface for water ionization [145].

$$\text{Photon activation: } TiO_2 + h\nu \rightarrow e^- + h^+$$

$$\text{Water ionization: } H_2O + h^+ \rightarrow OH^- + H^+$$

Since many reactive oxygen species are generated as an intermediate during the photoelectrochemical watersplitting reaction (Figure 16), both bulk and surface characteristics of the semiconductor will significantly influence the mechanism and kinetics of charge separation and interfacial charge transfer. Sun et al. proposed the photoelectrochemical watersplitting reaction pathway in Titania (Figure 17). According to them, water-splitting occurs by the formation of

hydroperoxide intermediate. Later, Ti–OH and Ti–OOH groups are formed due to nucleophilic attack of water following the coupling process and O–O bond formation. Then, it collapses to produce oxygen with regeneration of TiO_2 [146].

Figure 16. Reactive oxygen species generated in the photocatalytic oxidation steps of water. Reproduced from [146], Copyright 2017, American Chemical Society.

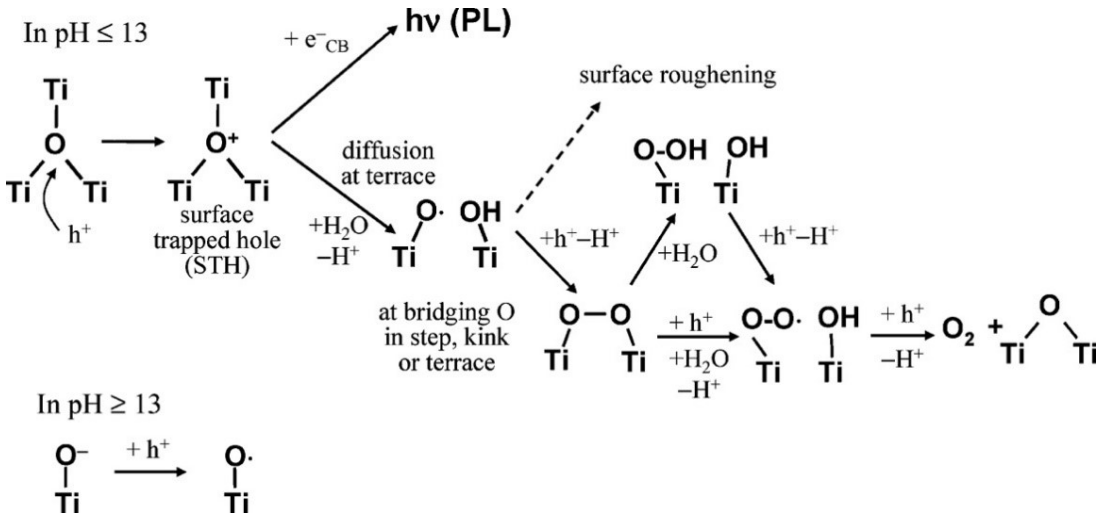

Figure 17. Photoelectrochemical watersplitting reaction mechanism in Titania. Reproduced from [146], Copyright 2007, American Chemical Society.

Thus, based on the overall reaction mechanism, the presence of $O_2^{\circ -}$ and OH^- on the semiconductor's surface are likely to be an active site for the photoelectrochemical water oxidation. The defective Titania is enriched with surface hydroxyl groups and as well, highly active species such as $O_2^{\circ -}$ and O_2^{2-} will be produced on Ti^{3+} site when it reacts with dissolved oxygen (Figure 18) [147,148]. Whereas pristine Titania will barely afford chemisorptions sites. Hence, point defects in reduced Titania act as a reactive center for photoelectrochemical water-splitting reaction.

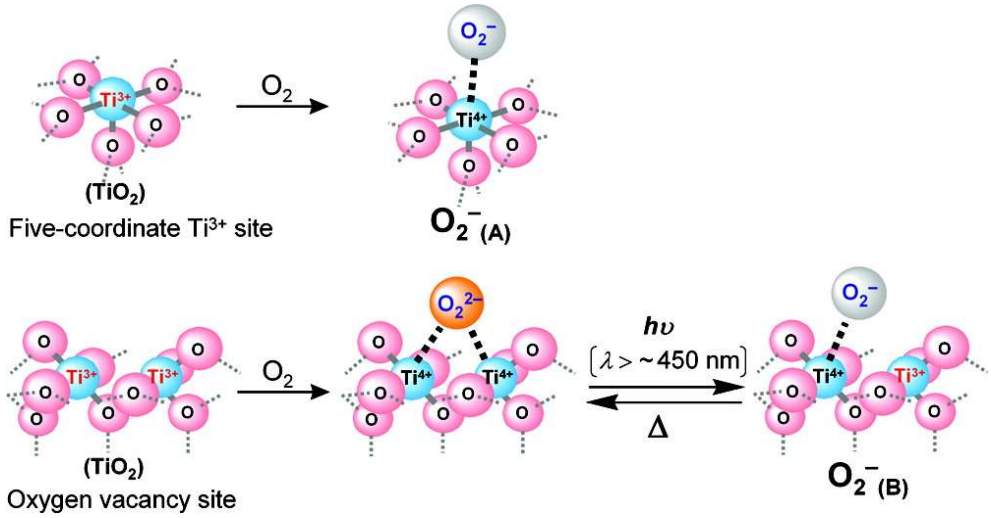

Figure 18. Surface reactivity of reduced Titania under visible light illumination. Reproduced from [147], Copyright 2010, American Chemical Society.

Apart from the surface phenomena, bulk characteristics of defective Titania like superficial and deep defect states offer a dominant pathway for charge transport [148–158]. Also, defective Titania absorbs visible light, and the defect concentration tunes their optical behavior [159–162]. Importantly, defective Titania possesses numerous dangling bonds and serve as a bridge to facilitate charge transfer once it is photo-excited. Thus, benefiting from the surface adsorption and bulk properties through point defects, reduced Titania could serve as an efficient photo-electrocatalyst and as a generic platform for other defective metal oxides.

9. Challenges in Reduced Titania

Point defects in reduced Titania are usually not stable in air, as Ti^{3+}/Ti^{2+} is easily oxidized and even susceptible to oxidation by dissolved oxygen in the water. Furthermore, the strategies to develop reduced Titania involve multiple steps, harsh synthesis conditions, or expensive facilities [69,162–168]. Therefore, developing a simple and economic strategy to synthesize stable reduced TiO_2 is still a great challenge. Besides, the control of the quality and quantity of defects during preparation is complicated. However, the optimal concentration of point defects in reduced Titania is essential for the best catalytic activity. At higher concentrations, it functions as an electron trap and in case of photo-electrochemical water-splitting it acts as a scatterer in electro-catalytic water-splitting [169]. Moreover, reduced Titania has mostly triclinic crystal symmetry with very similar lattice parameters. As a result, the formed material usually contains various sub-stoichiometries.

10. Applications

The diverse characteristics of reduced Titania such as robustness, electron richness, chemical inertness (stability), electrical conductivity, visible absorption makes them a suitable candidate for cathodic protection of steel in concrete, photodegradation of organic compounds, CO_2 reduction, Oxygen Reduction Reaction, solar cells, fuel cells, coating for tribological improvement, remediation of aqueous waste and contaminated water, electronic and optoelectronic devices, field emission, supercapacitors, microwave absorbers, photoelectrochemical sensor etc. [12,68,170–201]. It is also used as a chemical catalyst for ethylene polymerization, production of chemicals such as pyrite, glyoxylic acid and oxidation of flue gases, trichloroethylene. The enhanced catalytic activity has been frequently attributed to the presence of oxygen vacancies, $Ti^{3+/2+}$ species, hydroxyl groups, mid-gap energy levels. It also acts as a promising catalytic support for platinum and shows performance comparable to carbon black in PEM fuel cell technologies.

11. Towards Commercial Development

Currently, certain companies like Atranova, Atraverda, are in the process of making batteries, fuel cells with an electrically conductive titanium suboxide (Ti_4O_7) with the trade name Ebonex®. Lithium-ion rechargeable battery shows excellent rate performance with reduced Titania due to the oxygen vacancies, which creates well-balanced Li^+/e^- diffusion and provides short lithium-ion diffusion path and reduced charge diffusion resistance. Besides, the disordered surface of reduced Titania improves pseudocapacitive lithium storage. Vector Corrosion Technologies use titanium suboxides for cathodic protection of concrete [39–41].

12. Conclusions

Without a doubt, titanium sub-oxides with different crystal structures and colors have attracted tremendous interest due to their outstanding, electrical, optical and catalytic properties. The controlled oxygen vacancies in Titania impose significant structural modifications and substantially vary the conductivity from n-type to p-type semiconductors, and even quasi-metallic conductors. It also turns a colorless, inert Titania to a colorful, reactive defect-rich Titania. Despite the excellent electrical conductivity and visible absorption, their catalytic activity is still far from the ideal expectation. Thus, managing and optimizing the defects and the spatial distribution for catalytic activity is a critical issue. Different synthesis methods usually lead to various properties of defective titanium oxides. Importantly, much efforts and optimization are required to control the defects (n/p-type), concentration, and their spatial distribution. It is practically difficult to introduce defects of specific types into the desired location and at a controlled proportion, which requires more in-depth investigations. Also, new methods and tools must be developed to precisely characterize the defects in Titania lattice. For example, the atomic scale understanding, dynamics of defect, migration, and reconstruction of defects in Titania are still unexplored. The authors feel that the theoretical investigations and simulation methods will help to understand the structure–property relationship of defect-rich Titania. Besides, the proposed mechanism of catalytic activity in reduced TiO_2 should be evidenced through a more specific way. Also, it is of dire importance to consider the overall changes of the chemical environment in Titania rather than to focus locally on the defects, such as Ti^{3+} or V_O. However, comprehensively the defect-rich Titania will be a futuristic catalyst for water-splitting applications with a combinatorial attempt from materials scientists, physicists, and chemists.

Acknowledgments: S.J. thanks the Department of Science and Technology for the award of DST-INSPIRE Fellowship and Bhaskara Advanced Solar Energy (BASE) Internship.

Conflicts of Interest: The authors declare no conflict of interest.

References

1. Askeland, D.R.; Pradeep, P.F.; Wright, W.J. Imperfections in the atomic and Ionic Arrangements. In *The Science and Engineering of Materials*, 6th ed.; Global Engineering: Boston, MA, USA, 2014; pp. 113–145, ISBN 978-0-495-29602-7.
2. Heather, S. "DNA and Evolution" ThoughtCo. Available online: Thoughtco.com/dna-and-evolution-1224567 (accessed on 20 October 2018).
3. Hu, W.; Liu, Y.; Withers, R.L.; Frankcombe, T.J.; Norén, L.; Snashall, A.; Kitchin, M.; Smith, P.; Gong, B.; Chen, H.; et al. Electron-pinned defect-dipoles for high-performance colossal permittivity materials. *Nat. Mater.* **2013**, *12*, 821–826. [CrossRef] [PubMed]
4. Repp, S.; Weber, S.; Erdem, E. Defect evolution of nonstoichiometric ZnO Quantum Dots. *J. Phys. Chem. C* **2016**, *120*, 25124–25130. [CrossRef]
5. Hersam, M.C. Defects at the Two-Dimensional Limit. *J. Phys. Chem. Lett.* **2015**, *6*, 2738–2739. [CrossRef] [PubMed]

6. Martinez, U.; Hansen, J.; Lira, E.; Kristoffersen, H.H.; Huo, P.; Bechstein, R.; Lægsgaard, E.; Besenbacher, F.; Hammer, B.; Wendt, S. Reduced step edges on rutile TiO_2(110) as competing defects to oxygen vacancies on the terraces and reactive sites for ethanol dissociation. *Phys. Rev. Lett.* **2012**, *109*, 1–5. [CrossRef] [PubMed]
7. Cremer, T.; Jensen, S.C.; Friend, C.M. Enhanced photo-oxidation of formaldehyde on highly reduced o-TiO_2(110). *J. Phys. Chem. C* **2014**, *118*, 29242–29251. [CrossRef]
8. Sivula, K. Defects Give New Life to an Old Material: Electronically Leaky Titania as a Photoanode Protection Layer. *ChemCatChem* **2014**, *6*, 2796–2797. [CrossRef]
9. Gai-Boyes, P.L. Defects in Oxide Catalysts: Fundamental Studies of Catalysis in Action. *Catal. Rev.* **1992**, *34*, 1–54. [CrossRef]
10. Attariani, H.; Momeni, K.; Adkins, K. Defect Engineering: A Path toward Exceeding Perfection. *ACS Omega* **2017**, *2*, 663–669. [CrossRef]
11. Barzan, C.; Groppo, E.; Bordiga, S.; Zecchina, A. Defect Sites in H_2—Reduced TiO_2 Convert Ethylene to High Density Polyethylene without Activator. *ACS Catal.* **2014**, *4*, 986–989. [CrossRef]
12. Seo, H.; Park, C.J.; Cho, Y.J.; Kim, Y.B.; Choi, D.K. Correlation of band edge native defect state evolution to bulk mobility changes in ZnO thin films. *Appl. Phys. Lett.* **2010**, *96*, 65–68. [CrossRef]
13. Myung, S.-T.; Kikuchi, M.; Yoon, C.S.; Yashiro, H.; Kim, S.-J.; Sun, Y.-K.; Scrosati, B. Black anatase titania enabling ultra high cycling rates for rechargeable lithium batteries. *Energy Environ. Sci.* **2013**, *6*, 2609. [CrossRef]
14. Wang, X.; Huang, K.; Ma, W.; Cong, Y.; Ge, C.; Feng, S. Defect Engineering, Electronic Structure, and Catalytic Properties of Perovskite Oxide $La_{0.5}Sr_{0.5}CoO_{3-\delta}$. *Chem. A Eur. J.* **2017**, *23*, 1093–1100. [CrossRef] [PubMed]
15. Zhang, N.; Li, X.; Ye, H.; Chen, S.; Ju, H.; Liu, D.; Lin, Y.; Ye, W.; Wang, C.; Xu, Q.; et al. Oxide Defect Engineering Enables to Couple Solar Energy into Oxygen Activation. *J. Am. Chem. Soc.* **2016**, *138*, 8928–8935. [CrossRef] [PubMed]
16. Lin, Z.; Carvalho, B.R.; Kahn, E.; Lv, R.; Rao, R.; Terrones, H.; Pimenta, M.A.; Terrones, M. Defect engineering of two-dimensional transition metal dichalcogenides. *2D Mater.* **2016**, *3*, 1–21. [CrossRef]
17. Feng, H.; Xu, Z.; Ren, L.; Liu, C.; Zhuang, J.; Hu, Z.; Xu, X.; Chen, J.; Wang, J.; Hao, W.; et al. Activating Titania for Efficient Electrocatalysis by Vacancy Engineering. *ACS Catal.* **2018**, *8*, 4288–4293. [CrossRef]
18. Zhang, H.; Lv, R. Defect engineering of two-dimensional materials for efficient electrocatalysis. *J. Mater.* **2018**, *4*, 95–107. [CrossRef]
19. Chen, J.; Iyemperumal, S.K.; Fenton, T.; Carl, A.D.; Grimm, R.L.; Li, G.; Deskins, N.A. Synergy between Defects, Photoexcited Electrons, and Supported Single Atom Catalysts for CO_2 Reduction. *ACS Catal.* **2018**. [CrossRef]
20. Swaminathan, J.; Subbiah, R.; Singaram, V. Defect-Rich Metallic Titania ($TiO_{1.23}$)—An Efficient Hydrogen Evolution Catalyst for Electrochemical Water Splitting. *ACS Catal.* **2016**, *6*. [CrossRef]
21. Liu, C.; Zhang, A.Y.; Pei, D.N.; Yu, H.Q. Efficient Electrochemical Reduction of Nitrobenzene by Defect-Engineered TiO_{2-x} Single Crystals. *Environ. Sci. Technol.* **2016**, *50*, 5234–5242. [CrossRef]
22. Li, Y.H.; Liu, P.F.; Pan, L.F.; Wang, H.F.; Yang, Z.Z.; Zheng, L.R.; Hu, P.; Zhao, H.J.; Gu, L.; Yang, H.G. Local atomic structure modulations activate metal oxide as electrocatalyst for hydrogen evolution in acidic water. *Nat. Commun.* **2015**, *6*. [CrossRef]
23. Bak, T.; Nowotny, J.; Nowotny, M.K.; Sheppard, L.R. Defect engineering of titanium dioxide. *J. Aust. Ceram. Soc.* **2008**, *44*, 63–67. [CrossRef]
24. Lee, H.; Clark, S.J.; Robertson, J. Calculation of point defects in rutile TiO_2 by the Screened Exchange Hybrid Functional. *Phys. Rev. B* **2012**, *86*, 075209. [CrossRef]
25. Lu, T.C.; Wu, S.Y.; Lin, L.B.; Zheng, W.C. Defects in the reduced rutile single crystal. *Phys. B Condens. Matter* **2001**, *304*, 147–151. [CrossRef]
26. Eyert, V.; Schwingenschlogl, U.; Eckern, U. Charge order, orbital order, and electron localization in the Magneli phase Ti_4O_7. *Chem. Phys. Lett.* **2004**, *390*, 151–156. [CrossRef]
27. Wang, Z.W.; Shu, D.J.; Wang, M.; Ming, N. Ben Strain effect on diffusion properties of oxygen vacancies in bulk and subsurface of rutile TiO_2. *Surf. Sci.* **2012**, *606*, 186–191. [CrossRef]
28. Boonchun, A.; Reunchan, P.; Umezawa, N. Energetics of native defects in anatase TiO_2: A hybrid density functional study. *Phys. Chem. Chem. Phys.* **2016**, *18*, 30040–30046. [CrossRef]
29. Yagi, E.; Hasiguti, R.R.; Aono, M. Electronic conduction above 4 K of slightly reduced oxygen-deficient rutile TiO_{2-x}. *Phys. Rev. B* **1996**, *54*, 7945–7956. [CrossRef]

30. Finazzi, E.; Di Valentin, C.; Pacchioni, G.; Selloni, A. Excess electron states in reduced bulk anatase TiO_2: Comparison of standard GGA, GGA+U, and hybrid DFT calculations. *J. Chem. Phys.* **2008**, *129*. [CrossRef]
31. Diebold, U. The surface science of titanium dioxide. *Surf. Sci. Rep.* **2003**, *48*, 53–229. [CrossRef]
32. Bak, T.; Nowotny, J.; Rekas, M.; Sorrell, C.C. Defect chemistry and semiconducting properties of titanium dioxide: II. Defect diagrams. *J. Phys. Chem. Solids* **2003**, *64*, 1057–1067. [CrossRef]
33. Xiao, P.; Fang, H.; Cao, G.; Zhang, Y.; Zhang, X. Effect of Ti^{n+} defects on electrochemical properties of highly-ordered titania nanotube arrays. *Thin Solid Films* **2010**, *518*, 7152–7155. [CrossRef]
34. Agrawal, A.; Lin, J.; Barth, M.; White, R.; Zheng, B.; Chopra, S.; Gupta, S.; Wang, K.; Gelatos, J.; Mohney, S.E.; et al. Fermi level depinning and contact resistivity reduction using a reduced titania interlayer in n-silicon metal-insulator-semiconductor ohmic contacts. *Appl. Phys. Lett.* **2014**, *104*, 8–12. [CrossRef]
35. Nowotny, M.K.; Bak, T.; Nowotny, J. Electrical properties and defect chemistry of TiO_2 single crystal. II. Thermoelectric power. *J. Phys. Chem. B* **2006**, *110*, 16283–16291. [CrossRef] [PubMed]
36. Nowotny, J. Titanium dioxide-based semiconductors for solar-driven environmentally friendly applications: Impact of point defects on performance. *Energy Environ. Sci.* **2008**, *1*, 565–572. [CrossRef]
37. Santo, V.D.; Naldoni, A. *The Effect of Point Defects on the Ordered/Disorderd Morphology on the Electronic and Structural Features in the Black TiO_2 Nanomaterials*; World Scientific: Kansas city, KS, USA, 2017; Chapter 4; pp. 49–75, ISBN 978-1-78634-165-5.
38. Nowotny, J.; Alim, M.A.; Bak, T.; Idris, M.A.; Ionescu, M.; Prince, K.; Sahdan, M.Z.; Sopian, K.; Mat Teridi, M.A.; Sigmund, W. Defect chemistry and defect engineering of TiO_2-based semiconductors for solar energy conversion. *Chem. Soc. Rev.* **2015**, *44*, 8424–8442. [CrossRef] [PubMed]
39. Su, J.; Zou, X.; Chen, J.-S. Self-modification of titanium dioxide materials by Ti^{3+} and/or oxygen vacancies: New insights into defect chemistry of metal oxides. *RSC Adv.* **2014**, *4*, 13979–13988. [CrossRef]
40. Pan, X.; Yang, M.Q.; Fu, X.; Zhang, N.; Xu, Y.J. Defective TiO_2 with oxygen vacancies: Synthesis, properties and photocatalytic applications. *Nanoscale* **2013**, *5*, 3601–3614. [CrossRef]
41. Chen, X.; Liu, L.; Huang, F. Black titanium dioxide (TiO_2) nanomaterials. *Chem. Soc. Rev.* **2015**, *44*, 1861–1885. [CrossRef]
42. Fang, W.; Xing, M.; Zhang, J. Modifications on reduced titanium dioxide photocatalysts: A review. *J. Photochem. Photobiol. C Photochem. Rev.* **2017**, *32*, 21–39. [CrossRef]
43. Easteal, A.J.; Udy, D.J. Extraction of Titanium Dioxide (TiO_2) from Ilmenite and Titaniferous Slag. *J. Appl. Chem. Biotechnol.* **1973**, *23*, 865–870. [CrossRef]
44. Buettner, K.M.; Valentine, A.M. Bioinorganic chemistry of Titanium. *Chem. Rev.* **2012**, *112*, 1863–1881. [CrossRef] [PubMed]
45. Liu, L.; Chen, X. Titanium dioxide nanomaterials: Self-structural modifications. *Chem. Rev.* **2014**, *114*, 9890–9918. [CrossRef] [PubMed]
46. Seebauer, E.G.; Kratzer, M.C. Charged point defects in semiconductors. *Mater. Sci. Eng. R Rep.* **2006**, *55*, 57–149. [CrossRef]
47. Nowotny, J.; Bak, T.; Ali, M.A. Semiconducting Properties and Defect Disorder of Titanium Dioxide. *ECS Trans.* **2015**, *64*, 11–28. [CrossRef]
48. Bak, T.; Nowotny, J.; Nowotny, M.K.; Sheppard, L.R. Defect chemistry of titanium dioxide effect of interfaces. *J. Aust. Ceram. Soc.* **2007**, *43*, 49–55.
49. Nowotny, J.; Bak, T.; Burg, T. Electrical properties of polycrystalline TiO_2 at elevated temperatures. Electrical conductivity. *Phys. Status Solidi Basic Res.* **2007**, *244*, 2037–2054. [CrossRef]
50. Serpone, N. Is the band gap of pristine TiO_2 narrowed by anion- and cation-doping of titanium dioxide in second-generation photocatalysts? *J. Phys. Chem. B* **2006**, *110*, 24287–24293. [CrossRef] [PubMed]
51. Kuznetsov, V.N.; Serpone, N. On the Origin of the Spectral Bands in the Visible Absorption Spectra of Visible-Light-Active TiO_2 Specimens Analysis and Assignments. *J. Phys. Chem. C* **2009**, *113*, 15110–15123. [CrossRef]
52. Swaminathan, J.; Ravichandran, S. Insights into the Electrocatalytic Behavior of Defect-Centered Reduced Titania ($TiO_{1.23}$). *J. Phys. Chem. C* **2018**, *122*. [CrossRef]
53. Chen, J.; Lin, L.B.; Jing, F.Q. Theoretical study of F-type color center in rutile TiO_2. *J. Phys. Chem. Solids* **2001**, *62*, 1257–1262. [CrossRef]
54. Kittel, C. *Introduction to Solid State Physics*, 7th ed.; John Wiley & Sons: New York, NY, USA, 1996; pp. 585–595, ISBN 13: 9780471111818.

55. Morgan, B.J.; Watson, G.W. Intrinsic n-type Defect Formation in TiO_2: A Comparison of Rutile and Anatase from GGA+U Calculations. *J. Phys. Chem. C* **2010**, *114*, 2321–2328. [CrossRef]
56. Na-Phattalung, S.; Smith, M.F.; Kim, K.; Du, M.H.; Wei, S.H.; Zhang, S.B.; Limpijumnong, S. First-principles study of native defects in anatase TiO_2. *Phys. Rev. B Condens. Matter Mater. Phys.* **2006**, *73*, 1–6. [CrossRef]
57. Nowotny, M.K.; Sheppard, L.R.; Bak, T.; Nowotny, J. Defect Chemistry of Titanium Dioxide. Application of Defect Engineering in Processing of TiO_2 based photocatalysts. *J. Phys. Chem. C* **2008**, *112*, 5275–5300. [CrossRef]
58. Bak, T.; Burg, T.; Kang, S.J.L.; Nowotny, J.; Rekas, M.; Sheppard, L.; Sorrell, C.C.; Vance, E.R.; Yoshida, Y.; Yamawaki, M. Charge transport in polycrystalline titanium dioxide. *J. Phys. Chem. Solids* **2003**, *64*, 1089–1095. [CrossRef]
59. Kofstad, P. High-temperature oxidation of titanium. *J. Less Common Met.* **1967**, *12*, 449–464. [CrossRef]
60. Nowotny, J.; Bak, T.; Burg, T. Electrical properties of polycrystalline TiO_2. *Ionics* **2007**, *13*, 79–82. [CrossRef]
61. Tao, J.; Luttrell, T.; Batzill, M. A two-dimensional phase of TiO_2 with a reduced bandgap. *Nat. Chem.* **2011**, *3*, 296–300. [CrossRef]
62. Etacheri, V.; Seery, M.K.; Hinder, S.J.; Pillai, S.C. Oxygen rich titania: A dopant free, high temperature stable, and visible-light active anatase photocatalyst. *Adv. Funct. Mater.* **2011**, *21*, 3744–3752. [CrossRef]
63. Bowker, M.; Bennett, R.A. The role of Ti^{3+} interstitials in TiO_2(110) reduction and oxidation. *J. Phys. Condens. Matter* **2010**, *22*, 059801. [CrossRef]
64. Tanaka, T.; Sumiya, A.; Sawada, H.; Kondo, Y.; Takayanagi, K. Direct observation of interstitial titanium ions in TiO_2 substrate with gold nanoparticle. *Surf. Sci.* **2014**, *619*, 39–43. [CrossRef]
65. Tanaka, T.; Sano, K.; Ando, M.; Sumiya, A.; Sawada, H.; Hosokawa, F.; Okunishi, E.; Kondo, Y.; Takayanagi, K. Oxygen-rich Ti_{1-x} O_2 pillar growth at a gold nanoparticle-TiO_2 contact by O_2 exposure. *Surf. Sci.* **2010**, *604*, L75–L78. [CrossRef]
66. Ohwada, M.; Kimoto, K.; Mizoguchi, T.; Ebina, Y.; Sasaki, T. Atomic structure of titania nanosheet with vacancies. *Sci. Rep.* **2013**, *3*, 2801. [CrossRef] [PubMed]
67. Nowotny, M.K.; Bak, T.; Nowotny, J.; Sorrell, C.C. Titanium vacancies in nonstoichiometric TiO_2 single crystal. *Phys. Status Solidi Basic Res.* **2005**, *242*, 88–90. [CrossRef]
68. Zheng, Q.; Lee, H.-J.; Lee, J.; Choi, W.; Park, N.-B.; Lee, C. Electrochromic titania nanotube arrays for the enhanced photocatalytic degradation of phenol and pharmaceutical compounds. *Chem. Eng. J.* **2014**, *249*, 285–292. [CrossRef]
69. Wang, G.; Wang, H.; Ling, Y.; Tang, Y.; Yang, X.; Fitzmorris, R.C.; Wang, C.; Zhang, J.Z.; Li, Y. Hydrogen-Treated TiO_2 Nanowire Arrays for Photoelectrochemical Water Splitting. *Nano Lett.* **2011**, *11*, 3026–3033. [CrossRef] [PubMed]
70. Chen, X.; Liu, L.; Liu, Z.; Marcus, M.A.; Wang, W.-C.; Oyler, N.A.; Grass, M.E.; Mao, B.; Glans, P.-A.; Yu, P.Y.; et al. Properties of Disorder-Engineered Black Titanium Dioxide Nanoparticles through Hydrogenation. *Sci. Rep.* **2013**, *3*, 1510. [CrossRef]
71. Chen, X.; Liu, L.; Yu, P.Y.; Mao, S.S. Increasing solar absorption for photocatalysis with black hydrogenated titanium dioxide nanocrystals. *Science* **2011**, *331*, 746–750. [CrossRef]
72. Nakajima, T.; Nakamura, T.; Shinoda, K.; Tsuchiya, T. Rapid formation of black titania photoanodes: Pulsed laser-induced oxygen release and enhanced solar water splitting efficiency. *J. Mater. Chem. A* **2014**, *2*, 6762. [CrossRef]
73. Rahman, M.A.; Bazargan, S.; Srivastava, S.; Wang, X.; Abd-Ellah, M.; Thomas, J.P.; Heinig, N.F.; Pradhan, D.; Leung, K.T. Defect-rich decorated TiO_2 nanowires for super-efficient photoelectrochemical water splitting driven by visible light. *Energy Environ. Sci.* **2015**, *8*, 3363–3373. [CrossRef]
74. Wang, Z.; Yang, C.; Lin, T.; Yin, H.; Chen, P.; Wan, D.; Xu, F.; Huang, F.; Lin, J.; Xie, X.; et al. Visible-light photocatalytic, solar thermal and photoelectrochemical properties of aluminium-reduced black titania. *Energy Environ. Sci.* **2013**, *6*, 3007. [CrossRef]
75. Tang, C.; Zhou, D.; Zhang, Q. Synthesis and characterization of Magneli phases: Reduction of TiO_2 in a decomposed NH3 atmosphere. *Mater. Lett.* **2012**, *79*, 42–44. [CrossRef]
76. Simon, P.; Pignon, B.; Miao, B.; Coste-Leconte, S.; Leconte, Y.; Marguet, S.; Jegou, P.; Bouchet-Fabre, B.; Reynaud, C.; Herlin-Boime, N. N-doped titanium monoxide nanoparticles with TiO rock-salt structure, low energy band gap, and visible light activity. *Chem. Mater.* **2010**, *22*, 3704–3711. [CrossRef]

77. Takeuchi, T.; Fukushima, J.; Hayashi, Y.; Takizawa, H. Synthesis of Ti_4O_7 Nanoparticles by Carbothermal Reduction Using Microwave Rapid Heating. *Catalysts* **2017**, *7*, 65. [CrossRef]
78. Tominaka, S.; Tsujimoto, Y.; Matsushita, Y.; Yamaura, K. Synthesis of nanostructured reduced titanium Oxide: Crystal structure transformation maintaining nanomorphology. *Angew. Chem. Int. Ed.* **2011**, *50*, 7418–7421. [CrossRef]
79. Guan, S.; Hao, L.; Lu, Y.; Yoshida, H.; Pan, F.; Asanuma, H. Fabrication of oxygen-deficient TiO_2 coatings with nano-fiber morphology for visible-light photocatalysis. *Mater. Sci. Semicond. Process.* **2016**, *41*, 358–363. [CrossRef]
80. Zou, X.; Liu, J.; Su, J.; Zuo, F.; Chen, J.; Feng, P. Facile synthesis of thermal- and photostable titania with paramagnetic oxygen vacancies for visible-light photocatalysis. *Chem. A Eur. J.* **2013**, *19*, 2866–2873. [CrossRef] [PubMed]
81. Huang, S.S.; Lin, Y.H.; Chuang, W.; Shao, P.S.; Chuang, C.H.; Lee, J.F.; Lu, M.L.; Weng, Y.T.; Wu, N.L. Synthesis of High-Performance Titanium Sub-Oxides for Electrochemical Applications Using Combination of Sol-Gel and Vacuum-Carbothermic Processes. ACS Sustain. *Chem. Eng.* **2018**, *6*, 3162–3168. [CrossRef]
82. Sinhamahapatra, A.; Jeon, J.P.; Yu, J.S. A new approach to prepare highly active and stable black titania for visible light-assisted hydrogen production. *Energy Environ. Sci.* **2015**, *8*, 3539–3544. [CrossRef]
83. Grigorov, K.G.; Grigorov, G.I.; Drajeva, L.; Bouchier, D.; Sporken, R.; Caudano, R. Synthesis and characterization of conductive titanium monoxide films. Diffusion of silicon in titanium monoxide films. *Vacuum* **1998**, *51*, 153–155. [CrossRef]
84. Xiong, L.B.; Li, J.L.; Yang, B.; Yu, Y. Ti^{3+} in the surface of titanium dioxide: Generation, properties and photocatalytic application. *J. Nanomater.* **2012**, *2012*. [CrossRef]
85. Haubrich, J.; Kaxiras, E.; Friend, C.M. The role of surface and subsurface point defects for chemical model studies on TiO_2: A first-principles theoretical study of formaldehyde bonding on rutile TiO_2(110). *Chem. A Eur. J.* **2011**, *17*, 4496–4506. [CrossRef] [PubMed]
86. Li, G.; Li, L.; Zheng, J. Understanding the defect chemistry of oxide nanoparticles for creating new functionalities: A critical review. *Sci. China Chem.* **2011**, *54*, 876–886. [CrossRef]
87. Janotti, A.; Varley, J.B.; Rinke, P.; Umezawa, N.; Kresse, G.; Van de Walle, C.G. Hybrid functional studies of the oxygen vacancy in TiO_2. *Phys. Rev. B* **2010**, *81*, 085212. [CrossRef]
88. Naldoni, A.; Allieta, M.; Santangelo, S.; Marelli, M.; Fabbri, F.; Cappelli, S.; Bianchi, C.L.; Psaro, R.; Dal Santo, V. Effect of nature and location of defects on bandgap narrowing in black TiO_2 nanoparticles. *J. Am. Chem. Soc.* **2012**, *134*, 7600–7603. [CrossRef] [PubMed]
89. Parker, J.C.; Siegel, R.W. Raman Microprobe Study of Nanophase TiO_2 and Oxidation-Induced Spectral Changes. *J. Mater. Res.* **1990**, *5*, 1246–1252. [CrossRef]
90. Stoyanov, E.; Langenhorst, F.; Steinle-Neumann, G. The effect of valence state and site geometry on Ti $L_{3,2}$ and O K electron energy-loss spectra of Ti_xO_y phases. *Am. Mineral.* **2007**, *92*, 577–586. [CrossRef]
91. Parras, M.; Varela, Á.; Cortés-Gil, R.; Boulahya, K.; Hernando, A.; González-Calbet, J.M. Room-temperature ferromagnetism in reduced rutile $TiO_{2-\delta}$ nanoparticles. *J. Phys. Chem. Lett.* **2013**, *4*, 2171–2176. [CrossRef]
92. Walsh, F.C.; Wills, R.G.A. The continuing development of Magnéli phase titanium sub-oxides and Ebonex® electrodes. *Electrochim. Acta* **2010**, *55*, 6342–6351. [CrossRef]
93. Arif, A.F.; Balgis, R.; Ogi, T.; Iskandar, F.; Kinoshita, A.; Nakamura, K.; Okuyama, K. Highly conductive nano-sized Magnéli phases titanium oxide (TiO_x). *Sci. Rep.* **2017**, *7*, 3646. [CrossRef]
94. Watanabe, M. Raman spectroscopy of charge-ordered states in Magneli titanium oxides. *Phys. Status Solidi* **2009**, *6*, 260–263. [CrossRef]
95. Åsbrink, S.; Magnéli, A. Crystal structure studies on trititanium pentoxide, Ti_3O_5. *Acta Crystallogr.* **1959**, *12*, 575–581. [CrossRef]
96. Onoda, M. Phase Transitions of Ti_3O_5. *J. Solid State Chem.* **1998**, *136*, 67–73. [CrossRef]
97. Ovsyannikov, S.V.; Wu, X.; Shchennikov, V.V.; Karkin, A.E.; Dubrovinskaia, N.; Garbarino, G.; Dubrovinsky, L. Structural stability of a golden semiconducting orthorhombic polymorph of Ti_2O_3 under high pressures and high temperatures. *J. Phys. Condens. Matter* **2010**, 22. [CrossRef]
98. Wu, Y.; Zhang, Q.; Wu, X.; Qin, S.; Liu, J. High pressure structural study of β-Ti_3O_5: X-ray diffraction and Raman spectroscopy. *J. Solid State Chem.* **2012**, *192*, 356–359. [CrossRef]
99. Kao, C.H.; Yeh, S.W.; Huang, H.L.; Gan, D.; Shen, P. Study of the TiO to anatase transformation by thermal oxidation of Ti film in air. *J. Phys. Chem. C* **2011**, *115*, 5648–5656. [CrossRef]

100. Kostenko, M.G.; Lukoyanov, A.V.; Rempel, A.A. Electronic structure and stability of nonstoichiometric titanium monoxide TiO_y with structural vacancies in one of the sublattices. *Phys. Solid State* **2013**, *55*, 2108–2115. [CrossRef]
101. Bartkowski, S.; Neumann, M. Electronic structure of titanium monoxide. *Phys. Rev. B* **1997**, *56*, 10656–10667. [CrossRef]
102. Kostenko, M.G.; Lukoyanov, A.V.; Zhukov, V.P.; Rempel, A.A. Vacancies in ordered and disordered titanium monoxide: Mechanism of B1 structure stabilization. *J. Solid State Chem.* **2013**, *204*, 146–152. [CrossRef]
103. Barudzija, T.; Gusev, A.; Jugovic, D.; Marinovic-Cincovic, M.; Dramicanin, M.; Zdujic, M.; Jovalekic, C.; Mitric, M. Structural and magnetic properties of mechanochemically synthesized nanocrystalline titanium monoxide. *Hem. Ind.* **2012**, *66*, 309–315. [CrossRef]
104. Guo, C.; Jia, S.; Meng, W.; Zheng, H.; Jin, L.; Liu, Y.; Shi, J.; Wang, J. Orientation domains in vacancy-ordered titanium monoxide. *Acta Crystallogr. Sect. B Struct. Sci. Cryst. Eng. Mater.* **2013**, *69*, 589–594. [CrossRef]
105. Valeeva, A.A.; Rempel, A.A.; Sprengel, W.; Schaefer, H. Identification and study of vacancies in titanium monoxide by means of positron annihilation techniques. *Phys. Chem. Chem. Phys.* **2003**, *5*, 2304–2307. [CrossRef]
106. Fujimura, T.; Iwasaki, H.; Kkegawa, T.; Tsuchida, Y.; Shimomura, O.; Factory, P.; Corporation, K.S.; Iwasaki, H.; Kkegawa, T.; Tsuchida, Y.; et al. Structure changes in vacancy-rich titanium monoxide at high pressures and high temperatures. *High Press. Res.* **2006**, 37–41. [CrossRef]
107. Denker, S.P. Electronic properties of titanium monoxide. *J. Appl. Phys.* **1966**, *37*, 142–149. [CrossRef]
108. Gunda, N.S.H.; Puchala, B.; Van der Ven, A. Resolving phase stability in the Ti-O binary with first-principles statistical mechanics methods. *Phys. Rev. Mater.* **2018**, *2*, 033604. [CrossRef]
109. Jostsons, A.; McDougall, P.G. Fault Structures in Ti_2O. *Phys. Status Solidi* **1968**, *29*, 873–889. [CrossRef]
110. Wang, Q.; Fan, J.; Zhang, S.; Yun, Y.; Zhang, J.; Zhang, P.; Hu, J.; Wang, L.; Shao, G. In situ coupling of Ti_2O with rutile TiO_2 as a core-shell structure and its photocatalysis performance. *RSC Adv.* **2017**, *7*, 54662–54667. [CrossRef]
111. Burton, B.P.; Van De Walle, A. First principles phase diagram calculations for the octahedral-interstitial system αTiO_X, $0 \leq X \leq 1/2$. *Calphad* **2012**, *39*, 97–103. [CrossRef]
112. Hamdy, M.S.; Amrollahi, R.; Mul, G. Surface Ti^{3+}-containing (blue) titania: A unique photocatalyst with high activity and selectivity in visible light-stimulated selective oxidation. *ACS Catal.* **2012**, *2*, 2641–2647. [CrossRef]
113. Liu, G.; Yin, L.C.; Wang, J.; Niu, P.; Zhen, C.; Xie, Y.; Cheng, H.M. A red anatase TiO_2 photocatalyst for solar energy conversion. *Energy Environ. Sci.* **2012**, *5*, 9603–9610. [CrossRef]
114. Liu, G.; Yang, H.G.; Wang, X.; Cheng, L.; Lu, H.; Wang, L.; Lu, G.Q.; Cheng, H.M. Enhanced photoactivity of oxygen-deficient anatase TiO_2 sheets with dominant {001} facets. *J. Phys. Chem. C* **2009**, *113*, 21784–21788. [CrossRef]
115. Zhu, Q.; Peng, Y.; Lin, L.; Fan, C.M.; Gao, G.Q.; Wang, R.X.; Xu, A.W. Stable blue TiO_{2-x} nanoparticles for efficient visible light photocatalysts. *J. Mater. Chem. A* **2014**, *2*, 4429–4437. [CrossRef]
116. Mu, J.; Spiecker, E.; Schmuki, P. Black TiO_2 Nanotubes: Cocatalyst-Free Open-Circuit Hydrogen Generation. *Nano Lett.* **2014**, *14*, 3309–3313. [CrossRef]
117. Kuznetsov, V.N.; Emeline, A.V.; Rudakova, A.V.; Aleksandrov, M.S.; Glazkova, N.I.; Lovtcius, V.A.; Kataeva, G.V.; Mikhaylov, R.V.; Ryabchuk, V.K.; Serpone, N. Visible-NIR light absorption of titania thermochemically fabricated from titanium and its alloys; UV-and visible-light-induced photochromism of yellow titania. *J. Phys. Chem. C* **2013**, *117*, 25852–25864. [CrossRef]
118. Wang, H.; Lin, T.; Zhu, G.; Yin, H.; Lü, X.; Li, Y.; Huang, F. Colored titania nanocrystals and excellent photocatalysis for water cleaning. *Catal. Commun.* **2015**, *60*, 55–59. [CrossRef]
119. Kako, T.; Umezawa, N.; Xie, K.; Ye, J. Undoped visible-light-sensitive titania photocatalyst. *J. Mater. Sci.* **2013**, *48*, 108–114. [CrossRef]
120. Regonini, D.; Adamaki, V.; Bowen, C.R.; Pennock, S.R.; Taylor, J.; Dent, A.C.E. AC electrical properties of TiO_2 and Magnéli phases, Ti_nO_{2n-1}. *Solid State Ion.* **2012**, *229*, 38–44. [CrossRef]
121. Zhang, H.; Zhou, M.; Fu, Q.; Lei, B.; Lin, W.; Guo, H.; Wu, M.; Lei, Y. Observation of defect state in highly ordered titanium dioxide nanotube arrays. *Nanotechnology* **2014**, *25*, 275603. [CrossRef]
122. Nowotny, M.K.; Bak, T.; Nowotny, J. Electrical Properties and Defect Chemistry of TiO_2 Single Crystal. IV. Prolonged Oxidation Kinetics and Chemical Diffusion. *J. Phys. Chem. B* **2006**, *110*, 16270–16282. [CrossRef]

123. Santara, B.; Giri, P.K.; Imakita, K.; Fujii, M. Evidence for Ti Interstitial Induced Extended Visible Absorption and Near Infrared Photoluminescence from Undoped TiO_2 Nanoribbons: An In Situ Photoluminescence Study. *J. Phys. Chem. C* **2013**, *117*, 23402–23411. [CrossRef]
124. Kevane, C.J. Oxygen Vaccancies and Electrical conduction in Metal Oxides. *Phys. Rev.* **1964**, *133*, A1431. [CrossRef]
125. Hossain, F.M.; Murch, G.E.; Sheppard, L.; Nowotny, J. The Effect of Defect Disorder on the Electronic Structure of Rutile TiO_{2-x}. *Defect Diffus. Forum* **2006**, *251–252*, 1–12. [CrossRef]
126. Guo, Q.; Zhou, C.; Ma, Z.; Ren, Z.; Fan, H. Fundamental Processes in Surface Photocatalysis on TiO_2. In *Heterogeneous Photocatalysis—From Fundamentals to Green Applications*; Springer: London, UK; pp. 361–370, ISBN 978-3-662-48717-4.361-370.
127. Sekiya, T.; Yagisawa, T.; Kamiya, N.; Mulmi, D.D.; Kurita, S.; Murakami, Y.; Kodaira, T. Defects in anatase TiO_2 single crystal controlled by heat treatments. *J. Phys. Soc. Jpn.* **2004**, *73*, 703–710. [CrossRef]
128. Kitada, A.; Hasegawa, G.; Kobayashi, Y.; Kanamori, K.; Nakanishi, K.; Kageyama, H. Selective preparation of macroporous monoliths of conductive titanium oxides Ti_nO_{2n-1} (n = 2, 3, 4, 6). *J. Am. Chem. Soc.* **2012**, *134*, 10894–10898. [CrossRef] [PubMed]
129. Eder, D.; Kramer, R. Stoichiometry of titanium suboxide Part 2 Electric properties. *Phys. Chem. Chem. Phys.* **2003**, *5*, 1314–1319. [CrossRef]
130. Kieslich, G.; Burkhardt, U.; Birkel, C.S.; Veremchuk, I.; Douglas, J.E.; Gaultois, M.W.; Lieberwirth, I.; Seshadri, R.; Stucky, G.D.; Grin, Y.; et al. Enhanced thermoelectric properties of the n-type Magneli phase $WO_{2.90}$: Reduced thermal conductivity through microstructure engineering. *J. Mater. Chem. A* **2014**, *2*, 13492–13497. [CrossRef]
131. Nowotny, J.; Radecka, M.; Rekas, M. Semiconducting properties of undoped TiO_2. *J. Phys. Chem Solids* **1997**, *58*, 927–937. [CrossRef]
132. Shibuya, T.; Yasuoka, K.; Mirbt, S.; Sanyal, B. A systematic study of polarons due to oxygen vacancy formation at the rutile TiO(110) surface by GGA+U and HSE06 methods. *J. Phys. Condens. Matter* **2012**, *24*. [CrossRef] [PubMed]
133. Gono, P.; Wiktor, J.; Ambrosio, F.; Pasquarello, A. Surface Polarons Reducing Overpotentials in the Oxygen Evolution Reaction. *ACS Catal.* **2018**, *8*, 5847–5851. [CrossRef]
134. Gravelle, P.C.; Juillet, F.; Meriaudeau, P.; Teichner, S.J. Surface reactivity of reduced titanium dioxide. *Discuss. Faraday Soc.* **1971**, *52*, 140–148. [CrossRef]
135. Amakawa, K.; Sun, L.; Guo, C.; Hävecker, M.; Kube, P.; Wachs, I.E.; Lwin, S.; Frenkel, A.I.; Patlolla, A.; Hermann, K.; et al. How Strain Affects the Reactivity of Surface Metal Oxide Catalysts. *Angew. Chem. Int. Ed.* **2013**, *52*, 13553–13557. [CrossRef]
136. Horikoshi, S.; Minatodani, Y.; Tsutsumi, H.; Uchida, H.; Abe, M.; Serpone, N. Influence of lattice distortion and oxygen vacancies on the uv-driven/microwave-assisted TiO_2 photocatalysis. *J. Photochem. Photobiol. A Chem.* **2013**, *265*, 20–28. [CrossRef]
137. Aschauer, U.; He, Y.; Cheng, H.; Li, S.C.; Diebold, U.; Selloni, A. Influence of subsurface defects on the surface reactivity of TiO_2: Water on anatase (101). *J. Phys. Chem. C* **2010**, *114*, 1278–1284. [CrossRef]
138. Schaub, R.; Thostrup, P.; Lopez, N.; Lægsgaard, E.; Stensgaard, I.; Nørskov, J.K.; Besenbacher, F. Oxygen vacancies as active sites for water dissociation on rutile TiO_2(110). *Phys. Rev. Lett.* **2001**, *87*. [CrossRef] [PubMed]
139. Jensen, S.C.; Friend, C.M. The dynamic roles of interstitial and surface defects on oxidation and reduction reactions on titania. *Top. Catal.* **2013**, *56*, 1377–1388. [CrossRef]
140. Tilocca, A.; Selloni, A. Reaction pathway and free energy barrier for defect-induced water dissociation on the (101) surface of TiO_2-anatase. *J. Chem. Phys.* **2003**, *119*, 7445–7450. [CrossRef]
141. Petrik, N.G.; Kimmel, G.A. Reaction Kinetics of Water Molecules with Oxygen Vacancies on Rutile TiO_2(110). *J. Phys. Chem. C* **2015**, *119*, 23059–23067. [CrossRef]
142. Kolbrecka, K.; Przyluski, J. Sub-stoichiometric titanium oxides as ceramic electrodes for oxygen evolution-structural aspects of the voltammetric behaviour of Ti_nO_{2n-1}. *Electrochim. Acta* **1994**, *39*, 1591–1595. [CrossRef]
143. Shan, Z.; Archana, P.S.; Shen, G.; Gupta, A.; Bakker, M.G.; Pan, S. NanoCOT: Low-Cost Nanostructured Electrode Containing Carbon, Oxygen, and Titanium for Efficient Oxygen Evolution Reaction. *J. Am. Chem. Soc.* **2015**, *137*, 11996–12005. [CrossRef]

144. Zhang, Z.; Cao, K.; Yates, J.T. Defect-electron spreading on the TiO_2(110) semiconductor surface by water adsorption. *J. Phys. Chem. Lett.* **2013**, *4*, 674–679. [CrossRef]
145. Nosaka, Y.; Nosaka, A.Y. Generation and Detection of Reactive Oxygen Species in Photocatalysis. *Chem. Rev.* **2017**, *117*, 11302–11336. [CrossRef]
146. Imanishi, A.; Okamura, T.; Ohashi, N.; Nakamura, R.; Nakato, Y. Mechanism of water photooxidation, at n-TiO_2 (rutile) (110) and (100) surfaces: Dependence on solution pH. *J. Am. Chem. Soc.* **2007**, *2*, 11569–11578. [CrossRef] [PubMed]
147. Komaguchi, K.; Maruoka, T.; Nakano, H.; Imae, I.; Ooyama, Y.; Harima, Y. Electron-transfer reaction of oxygen species on TiO_2 nanoparticles induced by Sub-band-gap illumination. *J. Phys. Chem. C* **2010**, *114*, 1240–1245. [CrossRef]
148. Pan, L.; Wang, S.; Zou, J.J.; Huang, Z.F.; Wang, L.; Zhang, X. Ti^{3+}-defected and V-doped TiO_2 quantum dots loaded on MCM-41. *Chem. Commun.* **2014**, *50*, 988–990. [CrossRef]
149. Fujishima, A.; Zhang, X.; Tryk, D.A. TiO_2 photocatalysis and related surface phenomena. *Surf. Sci. Rep.* **2008**, *63*, 515–582. [CrossRef]
150. Di Paola, A.; Bellardita, M.; Palmisano, L.; Barbieriková, Z.; Brezová, V. Influence of crystallinity and OH surface density on the photocatalytic activity of TiO_2 powders. *J. Photochem. Photobiol. A Chem.* **2014**, *273*, 59–67. [CrossRef]
151. Radecka, M.; Trenczek-Zajac, A.; Zakrzewska, K.; Rekas, M. Effect of oxygen nonstoichiometry on photo-electrochemical properties of TiO_{2-x}. *J. Power Sources* **2007**, *173*, 816–821. [CrossRef]
152. Wheeler, D.A.; Ling, Y.; Dillon, R.J.; Fitzmorris, R.C.; Dudzik, C.G.; Zavodivker, L.; Rajh, T.; Dimitrijevic, N.M.; Millhauser, G.; Bardeen, C.; et al. Probing the nature of bandgap states in hydrogen-treated TiO_2 nanowires. *J. Phys. Chem. C* **2013**, *117*, 26821–26830. [CrossRef]
153. Lo, H.H.; Gopal, N.O.; Ke, S.C. Origin of photoactivity of oxygen-deficient TiO_2 under visible light. *Appl. Phys. Lett.* **2009**, *95*, 2007–2010. [CrossRef]
154. Zhuang, J.; Weng, S.; Dai, W.; Liu, P.; Liu, Q. Effects of interface defects on charge transfer and photoinduced properties of TiO_2 bilayer films. *J. Phys. Chem. C* **2012**, *116*, 25354–25361. [CrossRef]
155. Ma, S.; Huang, S.D.; Fang, Y.H.; Liu, Z.P. TiH Hydride Formed on Amorphous Black Titania: Unprecedented Active Species for Photocatalytic Hydrogen Evolution. *ACS Catal.* **2018**, *8*, 9711–9721. [CrossRef]
156. Wang, Y.; Sun, H.; Tan, S.; Feng, H.; Cheng, Z.; Zhao, J.; Zhao, A.; Wang, B.; Luo, Y.; Yang, J.; et al. Role of point defects on the reactivity of reconstructed anatase titanium dioxide (001) surface. *Nat. Commun.* **2013**, *4*, 1–8. [CrossRef]
157. Wan, Z.; Huang, G.F.; Huang, W.Q.; Jiao, C.; Yan, X.G.; Yang, Z.M.; Zhang, Q. The enhanced photocatalytic activity of Ti^{3+} self-doped TiO_2 by a reduction method. *Mater. Lett.* **2014**, *122*, 33–36. [CrossRef]
158. Zhou, X.; Liu, N.; Schmuki, P. Photocatalysis with TiO_2 Nanotubes: "Colorful" Reactivity and Designing Site-Specific Photocatalytic Centers into TiO_2 Nanotubes. *ACS Catal.* **2017**, *7*, 3210–3235. [CrossRef]
159. Choudhury, B.; Choudhury, A. Oxygen defect dependent variation of band gap, Urbach energy and luminescence property of anatase, anatase-rutile mixed phase and of rutile phases of TiO_2 nanoparticles. *Phys. E Low Dimens. Syst. Nanostruct.* **2014**, *56*, 364–371. [CrossRef]
160. Das, T.K.; Ilaiyaraja, P.; Mocherla, P.S.V.; Bhalerao, G.M.; Sudakar, C. Influence of surface disorder, oxygen defects and bandgap in TiO_2 nanostructures on the photovoltaic properties of dye sensitized solar cells. *Sol. Energy Mater. Sol. Cells* **2016**, *144*, 194–209. [CrossRef]
161. Pan, S.; Liu, X.; Guo, M.; Yu, S.F.; Huang, H.; Fan, H.; Li, G. Engineering the intermediate band states in amorphous Ti^{3+}-doped TiO_2 for hybrid dye-sensitized solar cell applications. *J. Mater. Chem. A* **2015**, *3*, 11437–11443. [CrossRef]
162. Bharti, B.; Kumar, S.; Lee, H.-N.; Kumar, R. Formation of oxygen vacancies and Ti^{3+} state in TiO_2 thin film and enhanced optical properties by air plasma treatment. *Sci. Rep.* **2016**, *6*, 32355. [CrossRef] [PubMed]
163. Saputera, W.H.; Mul, G.; Hamdy, M.S. Ti^{3+}-containing titania: Synthesis tactics and photocatalytic performance. *Catal. Today* **2015**, *246*, 60–66. [CrossRef]
164. Zhu, G.; Shan, Y.; Lin, T.; Zhao, W.; Xu, J.; Tian, Z.; Zhang, H.; Zheng, C.; Huang, F. Hydrogenated blue titania with high solar absorption and greatly improved photocatalysis. *Nanoscale* **2016**, *8*, 4705–4712. [CrossRef]
165. Wei, W.; Yaru, N.; Chunhua, L.; Zhongzi, X. Hydrogenation of TiO_2 nanosheets with exposed {001} facets for enhanced photocatalytc activity. *RSC Adv.* **2012**, *2*, 8286–8288. [CrossRef]

166. Ali, A.; Ruzybayev, I.; Yassitepe, E.; Karim, A.; Shah, S.I.; Bhatti, A.S. Phase transformations in the pulsed laser deposition grown TiO_2 thin films as a consequence of O_2 partial pressure and Nd doping. *J. Phys. Chem. C* **2015**, *119*, 11578–11587. [CrossRef]
167. Lepcha, A.; Maccato, C.; Mettenbörger, A.; Andreu, T.; Mayrhofer, L.; Walter, M.; Olthof, S.; Ruoko, T.P.; Klein, A.; Moseler, M.; et al. Electrospun Black Titania Nanofibers: Influence of Hydrogen Plasma-Induced Disorder on the Electronic Structure and Photoelectrochemical Performance. *J. Phys. Chem. C* **2015**, *119*, 18835–18842. [CrossRef]
168. Huang, C.N.; Bow, J.S.; Zheng, Y.; Chen, S.Y.; Ho, N.J.; Shen, P. Nonstoichiometric titanium oxides via pulsed laser ablation in water. *Nanoscale Res. Lett.* **2010**, *5*, 972–985. [CrossRef] [PubMed]
169. Forster, M.; Potter, R.J.; Ling, Y.; Yang, Y.; Klug, D.R.; Cowan, A.J. Oxygen deficient α-Fe_2O_3 photoelectrodes: A balance between enhanced electrical properties and trap-mediated losses. *Chem. Sci.* **2015**, *6*, 4009–4016. [CrossRef] [PubMed]
170. Zhou, W.; Li, W.; Wang, J.; Qu, Y.; Yang, Y.; Xie, Y.; Zhang, K.; Wang, L.; Fu, H.; Zhao, D. Ordered Mesoporous Black TiO_2 as Highly Efficient Hydrogen Evolution Photocatalyst. *J. Am. Chem. Soc.* **2014**, *136*, 9280–9283. [CrossRef]
171. Zhou, H.; Zhang, Y. Enhancing the capacitance of TiO_2 nanotube arrays by a facile cathodic reduction process. *J. Power Sources* **2013**, *239*, 128–131. [CrossRef]
172. Lin, T. Effective nonmetal incorporation in black titania with enhanced solar energy utilization. *Energy Environ. Sci.* **2014**, *6*. [CrossRef]
173. Cui, H.; Zhao, W.; Yang, C.; Yin, H.; Lin, T.; Shan, Y.; Xie, Y.; Gu, H.; Huang, F. Black TiO_2 nanotube arrays for high-efficiency photoelectrochemical water-splitting. *J. Mater. Chem. A* **2014**, 8612–8616. [CrossRef]
174. Wang, Z.; Yang, C.; Lin, T.; Yin, H.; Chen, P.; Wan, D.; Xu, F.; Huang, F.; Lin, J.; Xie, X.; et al. H-doped black titania with very high solar absorption and excellent photocatalysis enhanced by localized surface plasmon resonance. *Adv. Funct. Mater.* **2013**, *23*, 5444–5450. [CrossRef]
175. Pei, D.-N.; Gong, L.; Zhang, A.-Y.; Zhang, X.; Chen, J.-J.; Mu, Y.; Yu, H.-Q. Defective titanium dioxide single crystals exposed by high-energy {001} facets for efficient oxygen reduction. *Nat. Commun.* **2015**, *6*, 8696. [CrossRef]
176. Bonanni, S.; Aït-Mansour, K.; Harbich, W.; Brune, H. Effect of the TiO_2 reduction state on the catalytic CO oxidation on deposited size-selected Pt clusters. *J. Am. Chem. Soc.* **2012**, *134*, 3445–3450. [CrossRef] [PubMed]
177. Pan, X.; Yang, M.; Fu, X.; Zhang, N.; Xu, Y. Defective TiO_2 with oxygen vacancies: Synthesis, properties and photocatalytic applications. *Nanoscale* **2013**, *5*, 3601. [CrossRef]
178. Tan, L.L.; Ong, W.J.; Chai, S.P.; Goh, B.T.; Mohamed, A.R. Visible-light-active oxygen-rich TiO_2 decorated 2D graphene oxide with enhanced photocatalytic activity toward carbon dioxide reduction. *Appl. Catal. B Environ.* **2015**, *179*, 160–170. [CrossRef]
179. Ramchiary, A.; Samdarshi, S.K. Hydrogenation based disorder-engineered visible active N-doped mixed phase titania. *Sol. Energy Mater. Sol. Cells* **2015**, *134*, 381–388. [CrossRef]
180. Kumar, V.; Ntwaeaborwa, O.M.; Holsa, J.; Motaung, D.E.; Swart, H.C. The role of oxygen and titanium related defects on the emission of TiO_2: Tb^{3+} nano-phosphor for blue lighting applications. *Opt. Mater.* **2015**, *46*, 510–516. [CrossRef]
181. Kang, Q.; Cao, J.; Zhang, Y.; Liu, L.; Xu, H.; Ye, J. Reduced TiO_2 nanotube arrays for photoelectrochemical water splitting. *J. Mater. Chem. A* **2013**, *1*, 5766–5774. [CrossRef]
182. Su, J.; Zou, X.; Zou, Y.; Li, G.; Wang, P.; Chen, J. Porous Titania with Heavily Self-Doped Ti^{3+} for Specific Sensing of CO at Room Temperature. *Inorg. Chem.* **2013**, *52*, 5924–5930. [CrossRef] [PubMed]
183. Zhao, A.; Masa, J.; Xia, W. Oxygen-deficient titania as alternative support for Pt catalysts for the oxygen reduction reaction. *J. Energy Chem.* **2014**, *23*, 701–707. [CrossRef]
184. Zhou, H.; Zhang, Y. Electrochemically Self-Doped TiO_2 Nanotube Arrays for Supercapacitors. *J. Phys. Chem. C* **2014**, *118*, 5626–5636. [CrossRef]
185. Li, Y.; Weng, Y.; Zhang, J.; Ding, J.; Zhu, Y.; Wang, Q.; Yang, Y.; Cheng, Y.; Zhang, Q.; Li, P.; et al. Observation of superconductivity in structure-selected Ti_2O_3 thin films. *NPG Asia Mater.* **2018**, *10*, 522–532. [CrossRef]
186. Wei, X.; Skomski, R.; Balamurugan, B.; Sun, Z.G.; Ducharme, S.; Sellmyer, D.J. Magnetism of TiO and TiO_2 nanoclusters. *J. Appl. Phys.* **2009**, *105*. [CrossRef]

187. Han, X.; Huang, J.; Jing, X.; Yang, D.; Lin, H.; Wang, Z.; Li, P.; Chen, Y. Oxygen-Deficient Black Titania for Synergistic/Enhanced Sonodynamic and Photoinduced Cancer Therapy at Near Infrared-II Biowindow. *ACS Nano* **2018**, *12*, 4545–4555. [CrossRef] [PubMed]
188. Tan, L.L.; Ong, W.J.; Chai, S.P.; Mohamed, A.R. Band gap engineered, oxygen-rich TiO_2 for visible light induced photocatalytic reduction of CO_2. *Chem. Commun.* **2014**, *50*, 6923–6926. [CrossRef] [PubMed]
189. Chong, S.V.; Kadowaki, K.; Xia, J.; Idriss, H. Interesting magnetic behavior from reduced titanium dioxide nanobelts. *Appl. Phys. Lett.* **2008**, *92*, 1–4. [CrossRef]
190. Guillemot, F.; Porté, M.C.; Labrugère, C.; Baquey, C. Ti^{4+} to Ti^{3+} conversion of TiO_2 uppermost layer by low-temperature vacuum annealing: Interest for titanium biomedical applications. *J. Colloid Interface Sci.* **2002**, *255*, 75–78. [CrossRef] [PubMed]
191. Wu, Q.M.; Ruan, J.M.; Zhou, Z.C.; Sang, S.B. Magneli phase titanium sub-oxide conductive ceramic Ti_nO_{2n-1} as support for electrocatalyst toward oxygen reduction reaction with high activity and stability. *J. Cent. South Univ.* **2015**, *22*, 1212–1219. [CrossRef]
192. Li, X.; Zhu, A.L.; Qu, W.; Wang, H.; Hui, R.; Zhang, L.; Zhang, J. Magneli phase Ti_4O_7 electrode for oxygen reduction reaction and its implication for zinc-air rechargeable batteries. *Electrochim. Acta* **2010**, *55*, 5891–5898. [CrossRef]
193. Yang, Y.; Zhang, T.; Le, L.; Ruan, X.; Fang, P.; Pan, C.; Xiong, R.; Shi, J.; Wei, J. Quick and facile preparation of visible light-driven TiO_2 photocatalyst with high absorption and photocatalytic activity. *Sci. Rep.* **2014**, *4*, 7045. [CrossRef]
194. Liu, Y.; Xing, M.; Zhang, J. Ti^{3+} and carbon co-doped TiO_2 with improved visible light photocatalytic activity. *Chin. J. Catal.* **2014**, *35*, 1511–1519. [CrossRef]
195. Shahid, M.; Choi, S.Y.; Liu, J.; Kwon, Y.U. Reduced titania films with ordered nanopores and their application to visible light water splitting. *Bull. Korean Chem. Soc.* **2013**, *34*, 2271–2275. [CrossRef]
196. Ren, Y.; Li, J.; Yu, J. Enhanced electrochemical performance of TiO_2 by Ti^{3+} doping using a facile solvothermal method as anode materials for lithium-ion batteries. *Electrochim. Acta* **2014**, *138*, 41–47. [CrossRef]
197. Xia, T.; Zhang, W.; Wang, Z.; Zhang, Y.; Song, X.; Murowchick, J.; Battaglia, V.; Liu, G.; Chen., X. Amorphous carbon-coated TiO_2 nanocrysals for improved lithium-ion battery and photocatalytic performance. *Nano Energy* **2014**, *6*, 109–118. [CrossRef]
198. Liu, H.; Yang, W.; Ma, Y.; Yao, J. Extended visible light response of binary TiO_2-Ti_2O_3 photocatalyst prepared by a photo-assisted sol-gel method. *Appl. Catal. A Gen.* **2006**, *299*, 218–223. [CrossRef]
199. Yin, G.; Huang, X.; Chen, T.; Zhao, W.; Bi, Q.; Xu, J.; Han, Y.; Huang, F. Hydrogenated Blue Titania for Efficient Solar to Chemical Conversions: Preparation, Characterization, and Reaction Mechanism of CO_2 Reduction. *ACS Catal.* **2018**, *8*, 1009–1017. [CrossRef]
200. Yeh, Y.C.; Li, S.S.; Wu, C.C.; Shao, T.W.; Kuo, P.C.; Chen, C.W. Stoichiometric dependence of TiO_x as a cathode modifier on band alignment of polymer solar cells. *Sol. Energy Mater. Sol. Cells* **2014**, *125*, 233–238. [CrossRef]
201. Pan, S.S.; Lu, W.; Zhao, Y.H.; Tong, W.; Li, M.; Jin, L.M.; Choi, J.Y.; Qi, F.; Chen, S.G.; Fei, L.F.; et al. Self-doped rutile titania with high performance for direct and ultrafast assay of H_2O_2. *ACS Appl. Mater. Interfaces* **2013**, *5*, 12784–12788. [CrossRef]